AN ABSTRACT OF THE THESIS OF

CHEN, SHAW-SUN for the degree of Master of Science

in Forest Products presented on November 18, 1980

Title: Evaluation of Testing Procedures for Stiffness Properties of Plywood

Signature redacted for privacy.

Abstract approved: _____
Anton Polensek

Elastic properties of plywood panels are essential for predicting structural behavior of wood systems. The ASTM Standard D 3043-76 which evaluates the moduli of elasticity (MOE) of plywood, treats these panels as one dimensional beams instead of two-dimensional plates, which results in an overestimate of the MOE. Improved procedures for plywood testing and evaluation of experimental data are needed.

A new procedure was developed, which estimates MOE's of the plywood panel tested as plate from experimentally measured deflections, corresponding external load and panel dimensions. The accuracy of the procedure was compared to that of other methods available; eight plywood panels, tested first as simply supported plate, were gradually cut into smaller specimens and tested by three different methods. Tests showed that MOE's of individual panels, obtained by the developed procedure, were about 20% to 35% smaller than the corresponding

MOE's obtained according to the ASTM. The percentages given were not statistically verified, because too small a sample size was used in testing. The main reasons for this difference are the use of beam equation by the ASTM method and the local variation in MOE on plywood panels.

Evaluation of Testing Procedures for Stiffness Properties of Plywood

by

Chen, Shaw-Sun

A THESIS

submitted to

Oregon State University

in partial fulfillment of
the requirements for the
degree of

Master of Science

Completed November 18, 1980

Commencement June 1981

APPROVED:

Signature redacted for privacy.

Associate Professor of Forest Products
in charge of major

Signature redacted for privacy.

Head of Department of Forest Products

Signature redacted for privacy.

Dean of Graduate School

Date thesis is presented November 18, 1980

Typed by Linda S. Crooks for Chen, Shaw-Sun

COMMITTEE MEMBERS

Signature redacted for privacy.

A. Polensek

Signature redacted for privacy.

T. Kennedy

Signature redacted for privacy.

J. Wilson

Signature redacted for privacy.

M. Corden

ACKNOWLEDGMENTS

Thanks are first dedicated to my parents for encouraging me to study in this country and continuous encouragement through letters.

Special appreciation is extended to Professor Anton Polensek for his kindly assistance throughout this study. His guidance and suggestion in the past two years have made my study at Oregon State University fruitful and satisfactory.

Thanks are also extended to Professor T. C. Kennedy in the Mechanical Engineering Department for serving as my minor professor. Grateful thanks to the other members of my committee, Professor J. B. Wilson, and Professor M. E. Corden.

Thanks to Ken Bastendorff and Akay Hasan of the Forest Research Lab. at O.S.U. for their assistance with some technical problems encountered in this study.

TABLE OF CONTENTS

LIST OF FIGURES

LIST OF TABLES

EVALUATION OF TESTING PROCEDURES FOR STIFFNESS PROPERTIES OF PLYWOOD

I. INTRODUCTION

Softwood plywood is usually constructed of an odd number of plies positioned with the grain of two adjacent plies perpendicular to one another and rigidly glued into a composite plate. Because of perpendicular ply orientation, elastic properties of plywood are different in two mutually perpendicular directions. Materials exhibiting this type of behavior are known as orthogonally anisotropic, or orthotropic. Thus, general theory for orthotropic materials is directly applicable to plywood plate analysis.

The increasing use of plywood for building components in residential construction, such as roofs, ceilings, floors and walls calls for continuous improvements in defining plywood design properties. Because deflection most often governs design of building components, accurate estimates of the modulus of elasticity (MOE) of plywood is essential for safe and economic design of wood buildings. To develop accurate and easy-to-use design procedures, structural components made of plywood have to be tested. In the process of developing such procedures, elastic properties of each plywood sheet in components are often needed. Therefore, a non-destructive experimental method, which can accurately predict MOE's of the whole sheet, would be quite valuable.

At first, plywood MOE's were based on the static bending test of small strips, which had the apparent disadvantage of non-useability of the specimens after testing. Next, non-destructive testing

procedures of whole sheets were developed; one of them was adapted as an ASTM Standard, i.e. Standard D3043-76 (16). Method C of this standard is the pure bending test for large specimens (up to four by eight feet in size) which are assumed to act as beams. Its measured deflection and elastic constants are due to bending only and free of shear deformation effect. Method C also assures that the panels are bent into large deflection without introducing in-plane forces. However, the ASTM testing procedure treats the plywood sheet as a beam and overlooks the two-way action of a plywood sheet behaving as an orthotropic plate, i.e. it neglects that deformation in one direction can produce stresses in the perpendicular direction. Thus MOE's determined according to this standard are overestimated. In addition to the ASTM Standard D3043-76 and testing of plywood strips, other procedures for evaluation of plywood MOE's have been attempted. Each one resulted in different properties.

Thus, the main objective of this study is to investigate the accuracy of the most common ones of these procedures and comparing their advantages and disadvantages. Another objective is to develop a non-destructive testing procedure that is more accurate than the ASTM standard.

II. LITERATURE REVIEW

Existing testing methods for determination of elastic constants of solid wood and wood based materials such as plywood and composition board are thoroughly described in numerous research papers (3, 4, 5, 7, 10, 11, 12, 14, 19, 25). This section deals with those articles which describe recent methods of testing and evaluating elastic constants of plywood. Theoretical analysis, which has provided the basis for evaluation of test data in this investigation, is discussed in Chapter III.

Hoppmann (10) was one of the earlier investigators who applied the flexture theory of plates to determine the bending and twisting stiffness of orthotropic plates. His orthotropic plate model consisted of a rectangular isotropic plate, to which identical, evenly spaced stiffeners were attached parallel to both edges. The solution for this composite structure existed at that time. It proved to bend and twist approximately the same as an orthotropic plate of equivalent stiffness.

Huffington (11) extended Hoppmann's method by introducing terms for the elastic rigidity constants and geometrical configuration for the component parts of the stiffened plates. He determined elastic rigidity constant D_x, D_y, D_{xy} and D_1 of the differential equation of equilibrium. These constants provided a convenience in solving differential equation for plates; they were first introduced by Timoshenko (22) as:

$$D_x = \frac{E_x h^3}{12 (1 - \nu_{xy} \nu_{yx})}$$

$$D_y = \frac{E_y\, h^3}{12\,(1 - \nu_{xy}\,\nu_{yx})}$$

$$D_{xy} = \frac{G_{xy}\, h^3}{12\,(1 - \nu_{xy}\,\nu_{yx})}$$

$$D_1 = \frac{\nu_{xy}\, E_y\, h^3}{12\,(1 - \nu_{xy}\,\nu_{yx})} = \frac{\nu_{yx}\, E_x\, h^3}{12\,(1 - \nu_{xy}\,\nu_{yx})}$$

in which

E_x, E_y = MOE in x, y direction;

ν_{xy}; (ν_{yx}) = Poisson's ratio of strain in the y (x) axis to the strain in the x (y) axis for a normal stress in x (y) direction;

G_{xy} = Modulus of rigidity in xy plane; and

h = Plate thickness.

Hearmon (9) and Lekhnitsky (15) gave the following stress-displacement relations (Equation 2.1) for a plate under bending moments M_1 and M_2, and twisting moment $M_{12} = M_{21}$, applied as shown in Figure 2.1.

$$\frac{\partial^2 u_3}{\partial X_1^2} = \frac{-2}{h}\,(S_{11}\,\sigma_1 + S_{12}\,\sigma_2 + S_{16}\,\sigma_6)$$

$$\frac{\partial^2 u_3}{\partial X_1^2} = \frac{-2}{h}\,(S_{12}\,\sigma_1 + S_{22}\,\sigma_2 + S_{26}\,\sigma_6) \qquad (2.1)$$

$$\frac{\partial^2 u_3}{\partial X_1 \partial X_2} = \frac{-1}{h} (S_{16}\, \sigma_1 + S_{26}\, \sigma_2 + S_{66}\, \sigma_6)$$

in which

u_3 = displacement in X_3 direction;

σ_1; σ_2 = stress in X_1, X_2 direction respectively;

σ_6 = shear stress in X_1, X_2 plane; and

S_{ij} = elastic compliances in tensor notation

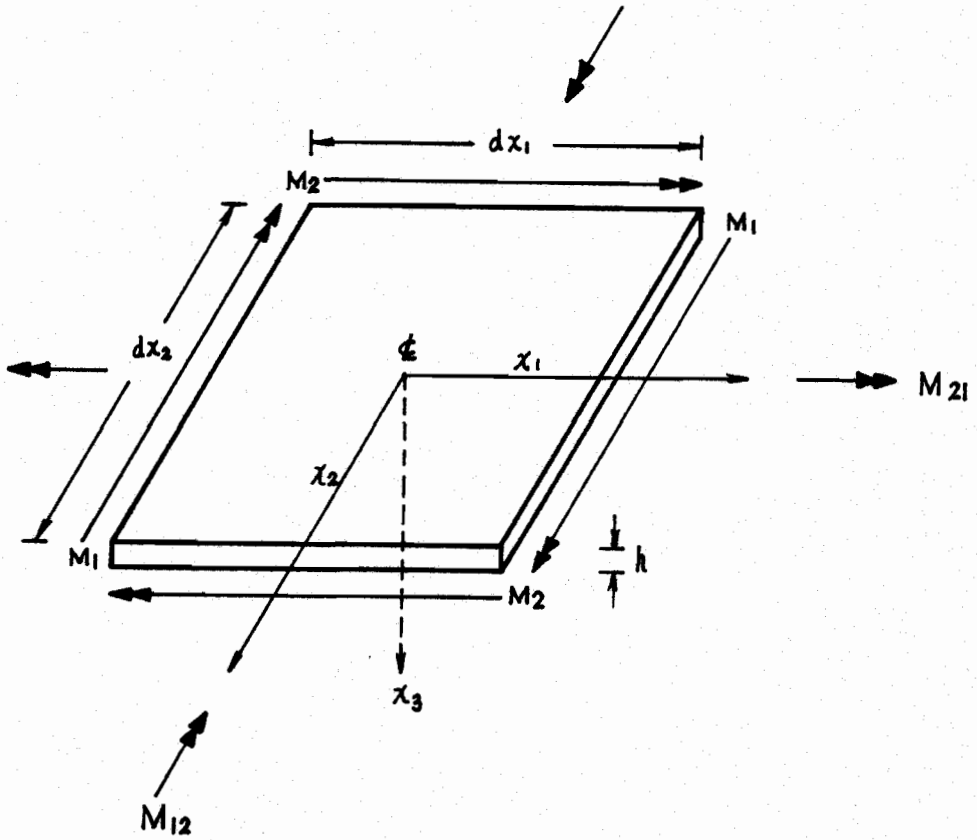

Figure 2.1. Differential plate element

The most general function which satisfies Equation 2.1 is:

$$u_3 = -\frac{\sigma_1}{h}(S_{11}X_1^2 + S_{12}X_2^2 + S_{16}X_1X_2) - \frac{\sigma_2}{h}(S_{21}X_1^2 +$$

$$S_{22}X_2^2 + S_{26}X_1X_2) - \frac{\sigma_6}{h}(S_{16}X_1^2 + S_{26}X_2^2 + S_{66}X_1X_2) +$$

$$C_1X_1 + C_2X_2 + C_3 \qquad (2.2)$$

The last three terms on the right hand side of Equation 2.2 relate to the position of the plate in the coordinate system; they can be omitted if the origin is located at the center of the plate. For pure bending and twisting, the maximum stresses are further simplified to:

$$\sigma_1 = \frac{6M_1}{h^2}$$

$$\sigma_2 = \frac{6M_1}{h^2}$$

$$\sigma_6 = \frac{6M_{12}}{h^2}$$

in which

$M_1 = M_2$ = bending moment per unit length; and

$M_{12} = M_{21}$ = twisting moment per unit length

Hearmon utilized a special plate testing arrangement (Figure 2.2A) to evaluate the elastic constants of plywood plate. He developed a "Hearmon's simplified equation" by letting $M_2 = M_{12} = 0$ in Equation 2.2:

$$u_3 = \frac{-6M_1}{h^3} (S_{11}X_1^2 + S_{12}X_2^2 + S_{16}X_1X_2) \qquad (2.4)$$

in which

$$M_1 = \text{constant} = \frac{P(a-b)}{4b}$$

However, important two-way bending effects which are caused by the triangular load pattern (asymmetrical loading arrangement as shown in Figure 2.2A) have been neglected (7). Considering the two-way bending would increase the overall deformation of the plate. Therefore, the value of elastic compliances according to this method are underestimated.

Another experimental method, developed by Hearmon and Adam (8) who followed suggestion by Thielemann, has been used for plywood, laminated plastics and stiffened plates. Witt, Hoppmann and Buxbaum (26) also used the same method to investigate elastic constants of anisotropic glass fabric laminates. The method involves the use of a rectangular and a square plate loaded as shown by Figures 2.2 A and B. S_{11} is found from simple bending theory, if deflection along the line AB is experimentally determined; S_{12} can be obtained from deflection along CD. Deflection measurements along the diagonal IJ and KL on the square plate yield S_{66}. S_{16} and S_{26} are based on deflections along EF and GH from bending tests and deflections along MN and OP from torsion respectively.

The principal elastic constants can be expressed by elastic compliance tensors as:

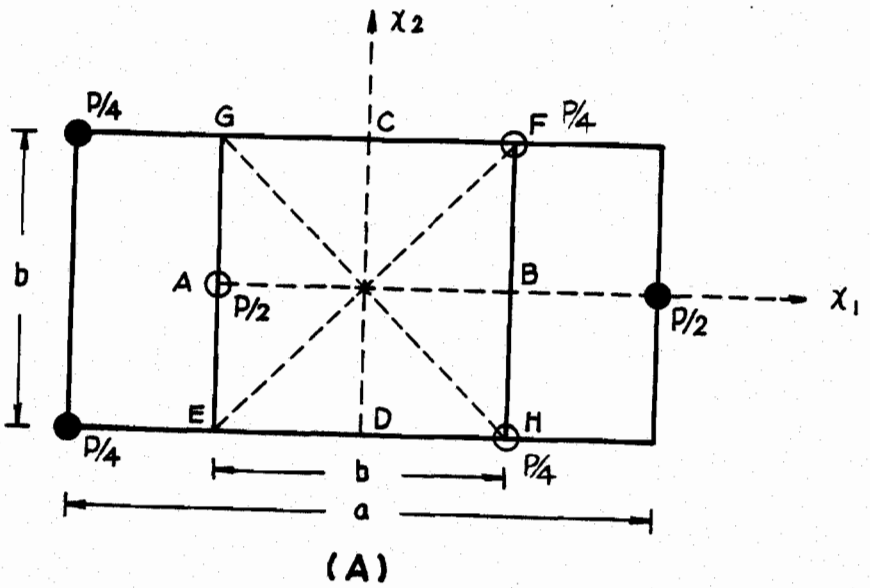

(A)

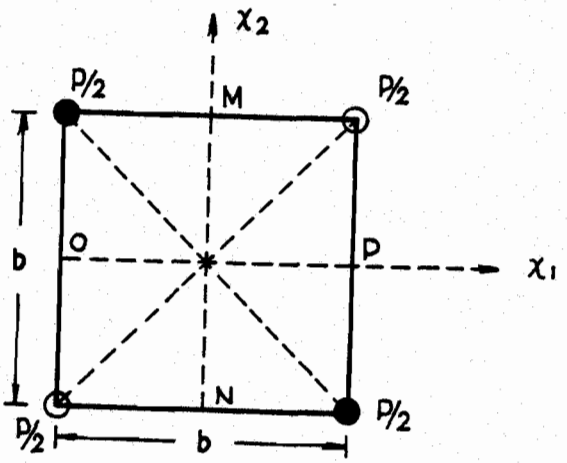

(B)

Solid circles represent downward concentrated forces of magnitude 1/2 p or 1/4 p as indicated and open circles represent upward concentrated forces.

Figure 2.2 (A). Plate in flexture.
(B). Plate in twisting.

$$E_x = \frac{1}{S_{11}} \tag{2.5}$$

$$E_y = \frac{1}{S_{22}} \tag{2.6}$$

$$\nu_{xy} = \frac{-S_{12}}{S_{11}} = - E_x S_{12} \tag{2.7}$$

$$\nu_{yx} = \frac{-S_{12}}{S_{22}} = - E_y S_{12} \tag{2.8}$$

$$G_{xy} = \frac{1}{S_{66}} \tag{2.9}$$

Hunt and Suddarth (12) developed a finite element technique for prediction of tensile modulus and Poisson's ratio of flakeboard. The prediction required the following inputs: MOE's along each orthotropic axis, two shear moduli and two Poisson's ratios for solid wood, specific gravity of wood particles and MOE of the binder. The determination of some of these properties is difficult and very cumbersome.

Ueda (24) developed a method for determining E_x, E_y, G_{xy} and ν_{xy} of plywood in terms of elastic constants of microlam (laminated veneer with plies oriented uniaxially). MOE's of the microlam beams were evaluated by bending and compressive tests according to ASTM standards (1). Shear moduli were based on the plate shear test and Poisson's ratios on compressive tests (24). Then the elastic constants for plywood, made of same veneers, were measured in the

same manner and compared to those based on microlams. His testing results showed the elastic properties of plywood except Poisson's ratio can be estimated with sufficient accuracy from the basic data of microlam. The plywood's MOE's are calculated by:

$$E_x = E_L A + E_T (1 - A) \tag{2.10}$$

$$E_y = E_T A + E_L (1 - A) \tag{2.11}$$

in which

$$A = \frac{I_\ell}{I}$$

I_ℓ = total moment of inertia of all veneer with grain parallel to face grain direction;

I = the moment of inertia of the full cross section; and

E_L (E_T) = MOE of longitudinal (tangential) direction for microlam

Shear modulus of plywood equalled:

$$G_{xy} = \sum_{i=1}^{n} G_{LT_i} t_i \tag{2.12}$$

in which

G_{LT} = shear modulus of LT plane for microlam;

t_i = thickness of veneer of i-th layer; and

n = number of plies.

Watanuki and Okuyama (25) applied the same procedure to investigate mechanical properties of two-species plywood and their relation

to the elastic constants of microlam. An important advantage of using Equations 2.10-2.12 to estimate plywood's elastic constants is that veneer properties of many species can be assumed to be equal to properties of clear wood and available in Wood Handbook (25). If clear wood properties are not available, testing of microlam specimen is necessary to determine E_L, E_T, G_{LT}, ν_{LT}. Manufacture of microlam is time consuming and the procedure is not very accurate, because microlam specimens are not truly representative of the whole plywood plate behavior.

In 1977, Lee and Biblis (14) modified Hearmon's method by replacing plate with strips bending, which is the method originally proposed by Tsai in 1965. They estimated E_x, E_y, G_{xy}, ν_{xy}, ν_{yx} of orthotropic plates in terms of elastic compliances; and the compliances S_{ij}'s can be determined accurately by one of the following two methods:

1) S_{11} is determined from bending test of plywood strip with grain orientation along the span. S_{66}, $(S_{22} - S_{12})$ and $(S_{11} - S_{12})$ are based on the deflection at centroid of twisted square plywood plate with 0°, 45°, -45° grain direction of face veneer with respect to the edges of the specimen.

2) S_{11} and S_{22} are calculated from bending tests of plywood strips with 0° and 90° grain direction of face veneer. S_{66} and $(S_{11} + S_{22} - 2S_{12})$ are determined from the deflections at loading corners of square plates with 0° and ± 45° orientations respectively.

Experimental verification of these two methods showed the first method had the better estimation. However, the experimental measurement by the second method is slightly easier than that of the first method.

While most researchers employed testing of small specimens, McLain and Bodig (19) described several non-destructive methods which can be used to evaluate the in-plane elastic constants of full size wood composite boards. Their testing method was important because it approximated elastic properties of full-size commercially made plywood sheets. However, their results may lack the accuracy because they calculate the MOE's according to simple beam equation.

III. THEORETICAL PROCEDURE

3.1 General Differential Equation for Orthotropic Plates

The derivation of the differential equation for the deflection is summarized next. For thin plates like plywood, the plate size is large compared with the thickness. The resulting state of stress is approximately plane, for which the generalized Hook's law equals (9):

$$\sigma_x = C_{11}\varepsilon_x + C_{12}\varepsilon_y + C_{16}\gamma_{xy} \tag{3.1}$$

$$\sigma_y = C_{12}\varepsilon_x + C_{22}\varepsilon_y + C_{26}\gamma_{xy} \tag{3.2}$$

$$\tau_{xy} = C_{16}\varepsilon_x + C_{26}\varepsilon_y + C_{66}\gamma_{xy} \tag{3.3}$$

in which

σ_x, σ_y = normal stress in x, y direction;

τ_{xy} = shear stress in x-y plane;

ε_x, ε_y = strain in x, y direction;

γ_{xy} = shear strain in x-y plane; and

C_{ij} = elastic stiffness in tensor notation.

Orthotropic materials have two perpendicular axes of elastic symmetry. If their symmetry axes coincide with the coordinate axes, $C_{16} = C_{26} = 0$, thus, Equations 3.1 to Equation 3.3 become:

$$\sigma_x = C_{11}\varepsilon_x + C_{12}\varepsilon_y \tag{3.4}$$

$$\sigma_y = C_{21}\varepsilon_x + C_{22}\varepsilon_y \tag{3.5}$$

$$\tau_{xy} = C_{66}\gamma_{xy} \tag{3.6}$$

in which

$$C_{11} = \frac{E_x}{1 - \nu_{xy}\nu_{yx}} \quad ;$$

$$C_{22} = \frac{E_y}{1 - \nu_{xy}\nu_{yx}} \quad ;$$

$$C_{12} = C_{21} = \frac{\nu_{xy}E_x}{1 - \nu_{xy}\nu_{yx}} = \frac{\nu_{xy}E_y}{1 - \nu_{xy}\nu_{yx}} \quad ;$$

$C_{66} = G_{xy}$; and

E_x, E_y, G_{xy}, ν_{xy}, ν_{yx} are defined earlier in the text.

The moment resultants are formulated by integration of Equations 3.4 to Equation 3.6 over the plate thickness:

$$M_x = \int \sigma_x \, z \, d \, z = -D_x \left(\frac{\partial^2 w}{\partial x^2} + \nu_{yx} \frac{\partial^2 w}{\partial y^2}\right) \tag{3.7}$$

$$M_y = -D_y \left(\frac{\partial^2 w}{\partial y^2} + \nu_{xy} \frac{\partial^2 w}{\partial x^2}\right) \tag{3.8}$$

$$M_{xy} = -D_{xy} \frac{\partial^2 w}{\partial x \, \partial y} \tag{3.9}$$

in which

z = distance from the neutral axis of plate;

M_x, M_y = bending moment along y and x direction;

M_{xy} = twisting moment;

$$D_x = \frac{h^3}{12} C_{11} = \frac{E_x h^3}{12 (1 - \nu_{xy}\nu_{yx})} \quad ;$$

$$D_y = \frac{h^3}{12} C_{22} = \frac{E_y h^3}{12 (1 - \nu_{xy}\nu_{yx})} \quad ; \text{ and}$$

$$D_{xy} = \frac{h^3}{12} C_{66} = \frac{G_{xy} h^3}{6}$$

Plate is in equilibrium if (16):

$$\frac{\partial Q_x}{\partial x} + \frac{\partial Q_y}{\partial y} + p\ (x, y) = 0 \qquad (3.10)$$

in which

Q_x, Q_y = shearing force in x and y direction; and

$p(x,y)$ = applied load.

$$Q_x = \frac{\partial M_x}{\partial x} + \frac{\partial M_{yx}}{\partial y} \qquad (3.11)$$

$$Q_y = \frac{\partial M_y}{\partial y} + \frac{\partial M_{xy}}{\partial x} \qquad (3.12)$$

$$M_{yx} = M_{xy} \qquad (3.13)$$

Equations 3.10 to Equation 3.13 can be combined into:

$$\frac{\partial^2 M_x}{\partial x^2} + 2 \frac{\partial^2 M_{xy}}{\partial x \partial y} + \frac{\partial^2 M_y}{\partial y^2} + p\ (x,y) = 0 \qquad (3.14)$$

The substitution of Equations 3.7 to Equation 3.9 into Equation 3.14 yields the general differential equation for orthotropic plates (21):

$$D_x \frac{\partial^4 w}{\partial x^2} + (2 D_{xy} + \nu_{yx} D_x + \nu_{xy} D_y) \frac{\partial^4 w}{\partial y^2 \partial x^2} + D_y \frac{\partial^4 w}{\partial y^4} =$$

$$p\ (x,y) \qquad (3.15)$$

Applying Betti's reciprocal theorem, $\nu_{xy} D_y = \nu_{yx} D_x$, to Equation 3.15 results in:

$$D_x \frac{\partial^4 w}{\partial x^4} + 2H \frac{\partial^4 w}{\partial x^2 \partial y^2} + D_y \frac{\partial^4 w}{\partial y^2} = p\ (x,y) \qquad (3.16)$$

in which, $H = \nu_{xy} D_y + D_{xy}$, is called the effective torsional rigidity. Equation 3.16 is often expressed in a simpler form (21):

$$\frac{\partial^4 w}{\partial x^4} + 2k \frac{\partial^4 w}{\partial x^2 \partial \eta^2} + \frac{\partial^4 w}{\partial \eta^4} = \frac{p\ (x,y)}{D_x} \qquad (3.17)$$

in which

$$k = \frac{H}{\sqrt{D_x D_y}} \quad ;$$

$$y = \frac{\eta}{m} \quad ; \text{ and}$$

$$m = \sqrt[4]{E_x / E_y}$$

3.2. Solution for Differential Plate Equation

Equation 3.16 is a fourth order nonhomogeneous differential equation, solution for displacement function w(x,y) depends not only on elastic properties of plate, but also on support conditions and types of loading. To meet the objectives of this study, the following two cases will be solved:

1) Plate with simply supported edges and concentrated load at center.
2) Plate with two opposite ends simply supported (the other two edges are free), and moments applied along these ends.

The solution for the first case will be used to develop a new predicting procedure for MOE's of full-size plywood sheet. Second case is the pure moment test which is the basis for the ASTM plywood test (1). In this study, plywood sheets will be tested under conditions simulating these two cases to provide the data for comparing existing procedures for plywood testing.

3.2.1. Plate With Simply Supported Edges and Concentrated Load at Center

There are several methods to solve this case. As shown by Swada and Ueda (21), Equation 3.16 can be solved rigorously by Fourier series. Masuda, et al. (16) applied finite difference method to find the deflection of a plate which had its elastic symmetry different from the axes of the coordinate system (i.e. $C_{16} \neq 0$, $C_{26} \neq 0$). The most well known is Navier solution (22); it is accurate and easy-to-use, especially when the edges are simply supported (17).

Navier solution for simply supported orthotropic plate is discussed next.

A load p(x,y) uniformly distributed over the area of UV (Figure 3.1) can be represented in the form of a double trigonometric series (22):

$$p(x,y) = \sum_{m=1}^{\infty} \sum_{n=1}^{\infty} A_{mn} \sin \frac{m\pi x}{a} \sin \frac{n\pi y}{b} \qquad (3.18)$$

where

A_{mn} = coefficient of the series; and

m, n = 1, 3, 5, . . .

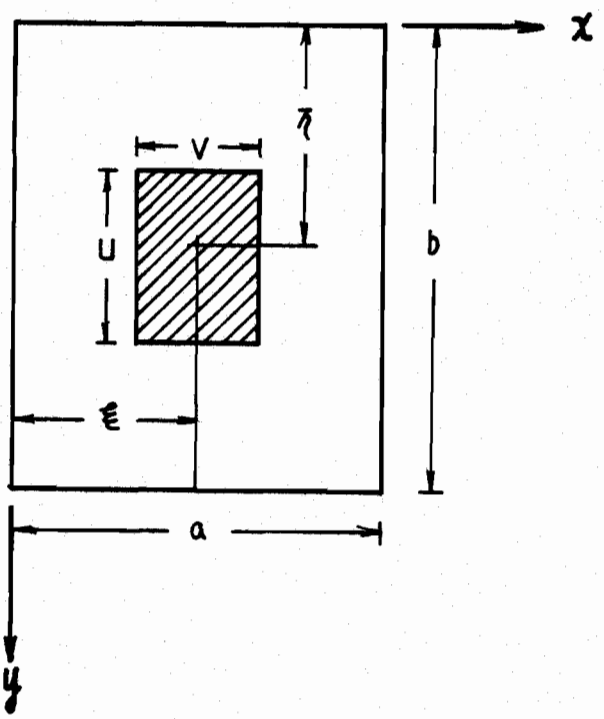

Figure 3.1. Plate with uniformly distributed load over the shaded area.

To calculate coefficients $A_{m'n'}$ for a certain loading condition, both sides of Equation 3.18 are multiplied by sin $(n'\pi y/b)dy$ and integrated from o to b to obtain

$$\int_o^b p(x,y) \sin \frac{n'\pi y}{b} dy = \frac{b}{2} \sum_{m=1}^{\infty} A_{mn'} \sin \frac{m\pi x}{a} \qquad (3.19)$$

Multiplying both sides of Equation 3.19 by sin $(m'\pi x/a)dx$ and integrating from o to a gives:

$$\int_o^a \int_o^b p(x,y) \sin \frac{m'\pi x}{a} \sin \frac{n'\pi y}{b} dx\, dy = \frac{ab}{4} A_{m'n'}$$

from which $A_{m'n'}$ is deduced:

$$A_{m'n'} = \frac{4}{ab} \int_o^a \int_o^b p(x,y) \sin \frac{m'\pi x}{a} \sin \frac{n'\pi y}{b} dx\, dy \qquad (3.20)$$

For the case of a single load, assumed to be uniformly distributed over the shaded area (Figure 3.1), Equation 3.20 becomes:

$$A_{mn} = \frac{4p}{abUV} \int_{\xi-U/2}^{\xi+U/2} \int_{\eta-V/2}^{\eta+V/2} \sin \frac{m\pi x}{a} \sin \frac{n\pi y}{b} dx\, dy$$

or

$$A_{mn} = \frac{16p}{\pi^2 mnUV} \sin \frac{m\pi\xi}{a} \sin \frac{n\pi\eta}{b} \sin \frac{m\pi U}{2a} \sin \frac{n\pi V}{2b} \qquad (3.21)$$

where ξ; η; U; V are defined in Figure 3.1.

A case of interest is a single concentrated load applied at any given point $x=\xi$, $y=\eta$. If in Equation 3.21 the load becomes concentrated, U and V go to zero, so that:

$$A_{mn} = \frac{4p}{ab} \sin \frac{m\pi\xi}{a} \sin \frac{n\pi\eta}{b} \tag{3.22}$$

Substituting Equation 3.22 into Equation 2.18 results in:

$$p(x,y) = \sum_{m=1}^{\infty} \sum_{n=1}^{\infty} \frac{4p}{ab} \sin \frac{m\pi\xi}{a} \sin \frac{n\pi\eta}{b} \sin \frac{m\pi x}{a} \sin \frac{n\pi y}{b} \tag{3.23}$$

Solution that satisfies Equation 3.16 is (17):

$$W(x,y) = \sum_{m=1}^{\infty} \sum_{n=1}^{\infty} W_{mn} \sin \frac{m\pi x}{a} \sin \frac{n\pi y}{b} \tag{3.24}$$

Thus, the derivative in Equation 3.24 are:

$$\frac{\partial^4 w}{\partial x^4} = \sum_{m=1}^{\infty} \sum_{n=1}^{\infty} \frac{m^4\pi^4}{a^4} W_{mn} \sin \frac{m\pi x}{a} \sin \frac{n\pi y}{b} \tag{3.25}$$

$$\frac{\partial^4 w}{\partial y^4} = \sum_{m=1}^{\infty} \sum_{n=1}^{\infty} \frac{m^4\pi^4}{b^4} W_{mn} \sin \frac{m\pi x}{a} \sin \frac{n\pi y}{b} \tag{3.26}$$

$$\frac{\partial^4 w}{\partial x^2 \partial y^2} = \sum_{m=1}^{\infty} \sum_{n=1}^{\infty} \frac{m^2 n^2 \pi^2}{a^2 b^2} W_{mn} \sin \frac{m\pi x}{a} \sin \frac{n\pi y}{b} \tag{3.27}$$

Substituting Equation 3.23, Equation 3.25 to Equation 3.27 into Equation 3.16 gives:

$$D_x \frac{\pi^4}{a^4} \sum_{m=1}^{\infty} \sum_{n=1}^{\infty} W_{mn} m^4 + 2H \frac{\pi^4}{a^2 b^2} \sum_{m=1}^{\infty} \sum_{n=1}^{\infty} W_{mn} n^2 m^2 +$$

$$D_y \frac{\pi^4}{b^4} \sum_{m=1}^{\infty} \sum_{n=1}^{\infty} W_{mn} n^4 = \frac{4p}{ab} \sum_{m=1}^{\infty} \sum_{n=1}^{\infty} \sin \frac{m\pi\xi}{a} \sin \frac{n\pi\eta}{b} \tag{3.28}$$

for which

$$W_{mn} = \frac{4p}{ab\pi^4} \frac{\sin \frac{m\pi\xi}{a} \sin \frac{n\pi\eta}{b}}{\frac{D_x}{a^4} m^4 + \frac{2H}{a^2b^2} m^2n^2 + \frac{D_y}{b^4} n^4} \tag{3.29}$$

Finally, substituting Equation 3.29 into Equation 3.24 results in:

$$W(x,y) = \frac{4p}{ab\pi^4} \sum_{m=1}^{\infty} \sum_{n=1}^{\infty} \frac{\sin \frac{m\pi\xi}{a} \sin \frac{n\pi\eta}{b} \sin \frac{m\pi x}{a} \sin \frac{n\pi y}{b}}{\frac{D_x}{a^4} m^4 + \frac{2Hm^2n^2}{a^2b^2} + \frac{D_y}{b^4} n^4} \tag{3.30}$$

If a concentrated load, p, is located at centroid:

$$W(x,y) = \frac{4p}{ab\pi^4} \sum_{m=1}^{\infty} \sum_{n=1}^{\infty} \frac{\sin \frac{m\pi}{2} \sin \frac{n\pi}{2} \sin \frac{m\pi x}{a} \sin \frac{n\pi y}{b}}{\frac{D_x}{a^4} m^4 + \frac{2Hm^2n^2}{a^2b^2} + \frac{D_y}{b^4} n^4} \tag{3.31}$$

This series converges rapidly and accurate deflection are obtained by considering only the first few terms. To check the accuracy, a computer program had been prepared, which allowed efficient computation of W(x,y) for various values of m and n. It showed that the difference of summation value between m = n = 9 and m = n = 25 is only 0.55%. Thus, in keeping the first five terms (m = n = 1, 3, 5, 7, 9) would be quite acceptable for this study.

3.2.2. Sensitivity Study: The Effect of Elastic Parameter On Deflection

The study is aimed at investigating how the potential inaccuracy of elastic constants affects theoretical plate deflection. For analytical convenience, a new variable, $R = E_x/E_y$, is introduced in Equation 3.38. This sensitivity study was done by changing one parameter at a time and repeating the analysis (Table 3.1). For each change, theoretical deflection value was compared to the control value, as indicated by the "% difference" in Table 3.1. The results do not reflect possible coupling effects, and changing independently only one parameter at a time may not represent a realistic condition. The control properties, based on the data in Wood Handbook (27), are associated with a 3/8" plywood sheet with E_x = 1752.6 Ksi; R = 2.005; G_{xy} = 89.3 Ksi and ν_{xy} = 0.449.

TABLE 3.1. RESULT OF SENSITIVITY STUDY

% difference / K	E_xxK	RxK	G_{xy}xK	ν_{xy}xK
0.5	+86.0	-40.97	+3.96	+0.46
0.7	+38.4	-23.54	+2.35	+0.29
0.9	+10.2	- 7.52	+0.79	+0.12
1	0	0	0	0
1.1	- 8.43	+ 7.31	-0.72	-0.05
1.3	-21.69	+21.1	-2.19	-0.23
1.5	-31.59	+33.98	-3.16	-0.40
1.7	-39.27	+46.04	-4.99	-0.58
1.9	-45.39	+57.36	-6.33	-0.76

Table 3.1 shows that inaccuracies of E_x and R greatly affect plate deflection. The effect of G_{xy} and ν_{xy} is minor; if G_{xy} ranges from 0.5 X G_{xy} to 1.9 X G_{xy} (Table 3.1), maximum plate deflection differs by less than 7%. The same variation for ν_{xy} produces the difference of less than 1%. Thus, approximate values for G_{xy} and ν_{xy}, such as those given in Wood Handbook (27), may be used for the plywood plate analysis or in the evaluation of E_x and R. The associated loss of accuracy for predicted E_x and R are expected to be negligible.

3.2.3. Inversion of Equation 3.31

This section describes the numerical method for inversion of Equation 3.31, a necessary step in predicting E_x and R in terms of W(x,y), plate dimensions, loading and tabulated values for G_{xy} and ν_{xy}. The inversion is accomplished by Newton's method of tangents (20). The root of a function, y = f(x), is given by successive approximation (20):

$$X_{n+1} = X_n - \frac{f(X_n)}{f'(X_n)} \tag{3.32}$$

in which

X_n = n-th approximation of root x;

X_{n+1} = (n+1)-th approximation;

$f(X_n)$ = the value of a function after n-th approximation of X_n; and

$f'(X_n)$ = first derivative of $f(X_n)$.

The general form of Equation 3.31 is $y = f(E_x, R, G_{xy}, \nu_{xy}, h, a, b, p)$ in which y and function f are known. Arguments G_{xy} and ν_{xy} can be obtained from handbooks and p, h, a and b follow from the plate configuration. Deflection y is assumed to be obtained experimentally. In order to apply Newton's method of tangent to solve for E_x and R, a modified method has been developed. Figure 3.2 shows the flow chart for the computer program prepared for this method. The principle of the procedure is iteration consisting of applying Equation 3.32 twice in succession to predict first E_x and then R. Therefore, two sets of deflection measurements, $W_{1_{(x_1,y_1)}}$ and $W_{2_{(x_2,y_2)}}$ are necessary: one for E_x, the other for R. To initialize iteration, reasonable values for E_x and R are first assumed to be E_{xo} and R_o. Their importance will be discussed more in detail in Section 5.2.2.

3.2.4. Plate with Opposite Ends Simply Supported and Moments Applied These Ends

Figure 3.3 depicts an orthotropic plate that is simply supported along the edges $x = \pm a/2$, and loaded by external moments which are uniformly distributed along the supports. Edges $y = o$ and $y = b$ are free.

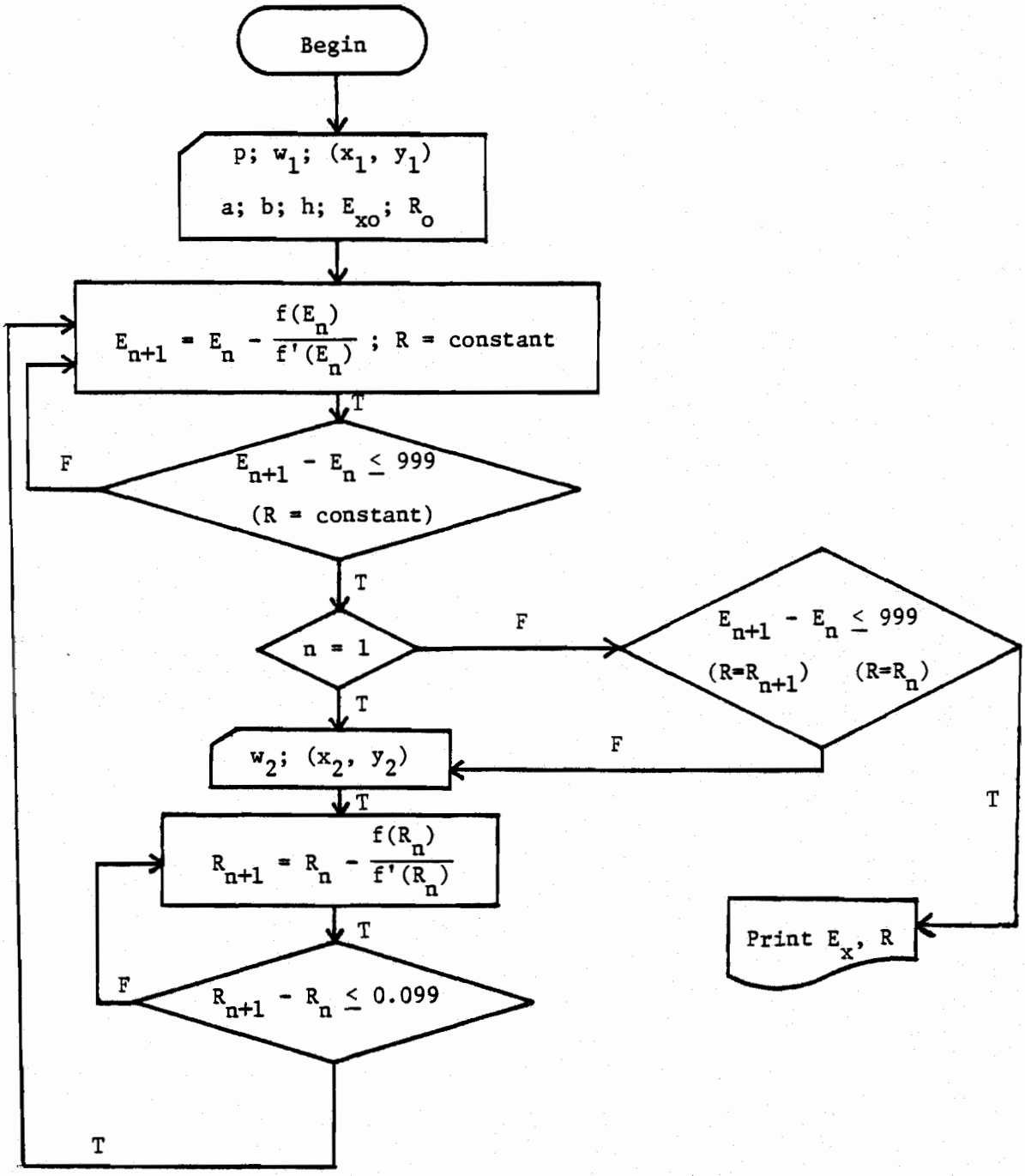

Figure 3.2. Flow chart of the Fortran IV program PLYMOE.

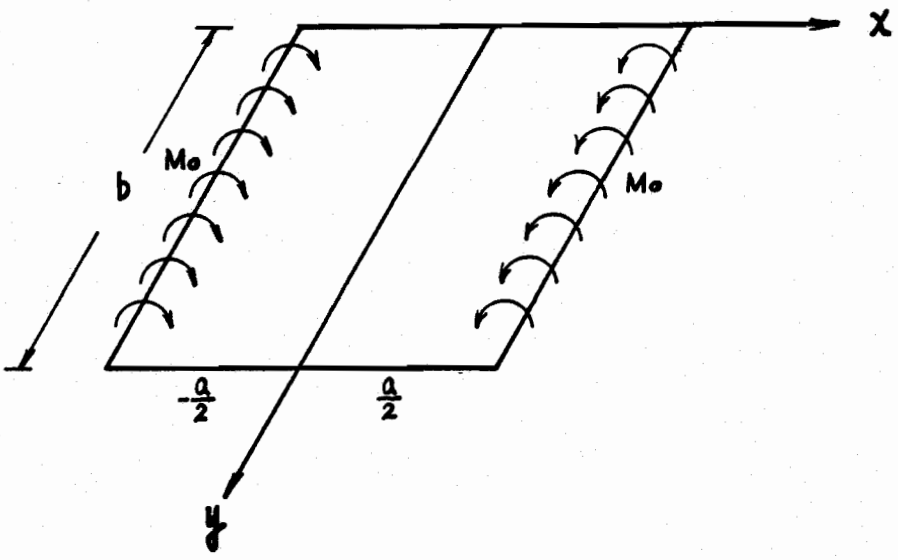

Figure 3.3. Plate under uniform bending moments of intensity M_o.

The deflection of this plate must satisfy the following homogeneous differential equation:

$$D_x \frac{\partial^4 w}{\partial x^4} + 2H \frac{\partial^4 w}{\partial x^2 \partial y^2} + D_y \frac{\partial^4 w}{\partial y^4} = 0 \tag{3.33}$$

and boundary conditions (17):

$$w = 0 \quad \text{for} \quad x = \pm a/2 \tag{3.34}$$

$$\left(\frac{\partial^2 w}{\partial y^2} + \nu_{xy} \frac{\partial^2 w}{\partial x^2} \right)_{y = 0,b} = 0 \tag{3.35}$$

$$- D_x \left(\frac{\partial^2 w}{\partial x^2}\right)_{x = \pm a/2} = M_y \tag{3.36}$$

Levy solution (17) for given conditions is:

$$W = \sum_{m=1}^{\infty} X_m \sin \frac{m\pi y}{b} \tag{3.37}$$

which satisfies the boundary condition (3.35) along the free edges. X_m is an arbitrary function of x. Substitution of Equation 3.37 into 3.33 yields:

$$\sum_{m=1}^{\infty} \left[D_x \left(\frac{\partial^4 X_m}{\partial x^4}\right) - 2H \left(\frac{\partial^2 X_m}{\partial x^2}\right) \left(\frac{m\pi}{b}\right)^2 + D_y \left(\frac{m\pi}{b}\right)^4 X_m\right] \sin \frac{m\pi y}{b} = 0 \tag{3.38}$$

If Equation 3.38 is to be satisfied for all values of y, then:

$$D_x \left(\frac{\partial^4 X_m}{\partial x^4}\right) - 2H \left(\frac{\partial^2 X_m}{\partial x^2}\right) \left(\frac{m\pi}{b}\right)^2 + D_y \left(\frac{m\pi}{b}\right)^4 X_m = 0 \tag{3.39}$$

Equation 3.39 is an ordinary differential equation with constant coefficients which have a solution in the form:

$$X_m = ce^{\lambda x} \tag{3.40}$$

in which c and λ are constants. Substitution of Equation 3.40 into Equation 3.39 leads to a characteristic equation:

$$D_x \lambda^4 - 2H\lambda^2 \left(\frac{m\pi}{b}\right)^2 + D_y \left(\frac{m\pi}{b}\right)^4 = 0 \tag{3.41}$$

which has the following roots:

$$\lambda_1 = \frac{m\pi}{b}\sqrt{\frac{1}{D_x}\left(H + \sqrt{H^2 - D_x D_y}\right)}$$

$$\lambda_2 = \frac{m\pi}{b}\sqrt{\frac{1}{D_x}\left(H - \sqrt{H^2 - D_x D_y}\right)}$$

$$\lambda_3 = -\lambda_1$$

$$\lambda_4 = -\lambda_2$$

For plywood the value of $(H^2 - D_x D_y)$ is less than zero (2), which results in complex roots, $(s \pm ti)$ and $(-s \pm ti)$. For instance, λ_1 becomes:

$$\lambda_1 = \frac{m\pi}{b}\sqrt{\frac{H + \sqrt{D_x D_y - H^2 i}}{D_x}} = \frac{m\pi}{b}\frac{1}{\sqrt{D_x}}\left(\cos\frac{\theta}{2} + i \sin\frac{\theta}{2}\right)$$

Thus

$$s = \frac{m\pi}{b}\frac{1}{\sqrt{D_x}}\cos\frac{\theta}{2}$$

$$t = \frac{m\pi}{b}\frac{1}{\sqrt{D_x}}\sin\frac{\theta}{2}$$

$$\theta = \tan^{-1}\left(\frac{\sqrt{D_x D_y - H^2}}{H}\right)$$

Now, the solution of Equation 3.41 can be written as:

$$X_m = (c_1 \cos \frac{m\pi tx}{b} + c_2 \sin \frac{m\pi tx}{b}) \cosh \frac{m\pi sx}{b} +$$

$$(c_3 \cos \frac{m\pi tx}{b} + c_4 \sin \frac{m\pi tx}{b}) \sinh \frac{m\pi sx}{b} \qquad (3.42)$$

In Figure 3.3., the moments are applied symmetrically, so that X_m must be an even function of x, which results in $c_2 = 0$ and $c_3 = 0$.

Inserting Equation 3.42 into Equation 3.37 gives:

$$W = \sum_{m=1}^{\infty} [c_1 (\cos \frac{m\pi tx}{b} \cosh \frac{m\pi sx}{b}) + c_4 (\sin \frac{m\pi tx}{b} \sinh \frac{m\pi sx}{b})]$$

$$\sin \frac{m\pi y}{b} \qquad (3.43)$$

which fully satisfies Equation 3.33.

The constant c_1, c_4 are determined from boundary conditions. Boundary condition of Equation 3.34 yields:

$$c_4 = -c_1 \cot (\frac{m\pi ta}{2b}) \coth (\frac{m\pi sa}{2b})$$

and the deflection becomes:

$$W = \sum_{m=1}^{\infty} c_1 [(\cos \frac{m\pi tx}{b} \cosh \frac{m\pi sx}{b}) - \coth \alpha \cot \beta (\sin \frac{m\pi tx}{b}$$

$$\sinh \frac{m\pi sx}{b})] \sin \frac{m\pi y}{b} \qquad (3.44)$$

in which

$$\alpha = \frac{m\pi sa}{2b} \text{ ; and}$$

$$\beta = \frac{m\pi ta}{2b} \text{ .}$$

The boundary condition of Equation 3.36 is used to determine constant c_1. To apply this condition a uniform bending moment along the edges ± a/2 is represented by a trigonometric series

$$M_y = \sum_{m=1}^{\infty} E_m \sin \frac{m\pi y}{b} \tag{3.45}$$

in which E_m is coefficient of series.

Substituting Equations 3.45 and 3.44 into Equation 3.36 gives

$$c_1 = \frac{-b^4 E_m}{m^4 \pi^4 [\Delta]} \tag{3.46}$$

where

$$[\Delta] = [\cosh \alpha \cos \beta (\cos \theta - \sin \theta \coth \alpha \cot \beta) -$$

$$\sinh \alpha \sin \beta (\sin \theta + \cos \theta \coth \alpha \cot \beta)].$$

For uniform bending moments of intensity M_o, Equation 3.45 becomes (22):

$$M_y = \frac{4M_o}{\pi} \sum_{m=1,3,5}^{\infty} \frac{1}{m} \sin \frac{m\pi y}{b} \tag{3.47}$$

Substituting Equation 3.46 and Equation 3.47 into Equation 3.44 yields the general expression for deflection of plate given in Fig. 3.3:

$$W = \frac{4M_o b^4}{\pi^5} \sum_{m=1,3,5}^{\infty} \frac{\sin \frac{m\pi y}{b}}{m^5[\Delta]} [\coth \alpha \cot \beta \left(\sin \frac{m\pi tx}{b} \right.$$

$$\left. \sinh \frac{m\pi sx}{b}\right) - \cos \frac{m\pi tx}{b} \cosh \frac{m\pi sx}{b}] \qquad (3.48)$$

The deflection along the axis of symmetry (x = 0) is:

$$W_{(x=0)} = \frac{4M_o b^4}{\pi^5} \sum_{m=1,3,5}^{\infty} \frac{- \sin \frac{m\pi y}{b}}{m^5[\Delta]} \qquad (3.49)$$

IV. EXPERIMENTAL PROCEDURE

4.1. Material Selection

Altogether eight plywood sheets, four ft. wide and eight ft. long, were purchased from local lumber yards. Six sheets were unsanded sheathing grade plywood with minimum veneer quality of C for face and D for back. These sheets had the following thicknesses: 3/8-inch (two sheets), 1/2-inch (two sheets) and 3/4-inch (two sheets). Additional two full sheets of 1/2-inch thickness were of marine grade plywood which were sanded on both sides. All the sheets were of five-ply construction, except for the 3/8-inch sheets which had three plies.

4.2. Testing of Full-size Plywood Sheets Under Concentrated Load

In this paper, term "full-sheet test" refers to the testing described in this section.

4.2.1. Testing Apparatus and Arrangement

An existing testing frame, that is a panel tester of the Forest Research Laboratory, Oregon State University, was used to apply concentrated load to the panels. To simulate the simply supported boundary conditions along all four edges, six-inch section of one-inch steel pipe were placed continuously between the frame and the sheet at a distance of one inch from each edge. These sections enabled the panel to freely move in both x- and y-direction.

Several sheets were slightly warped. To make sure that the sheets continuously supported on the pipes, two-inch steel pipes of 50-inch length were added on top of the panel along the four-foot edges and held down by adjustable angle iron (Figure 4.1). The 50-inch steel pipes were adjusted before each test, were free to roll and held the sheet to the support without causing in-plane forces. A 1000-pound load cell was attached to a loading cylinder (Figure 4.1) which received compressed oil from an identical cylinder placed in a Tinius Olsen testing machine. As the head of the testing machine moved down, the load cell, attached to the ram of the loading cylinder pushed on the steel disc of a three-inch diameter, which was placed onto the panel centroid to avoid punching a hole through the plywood.

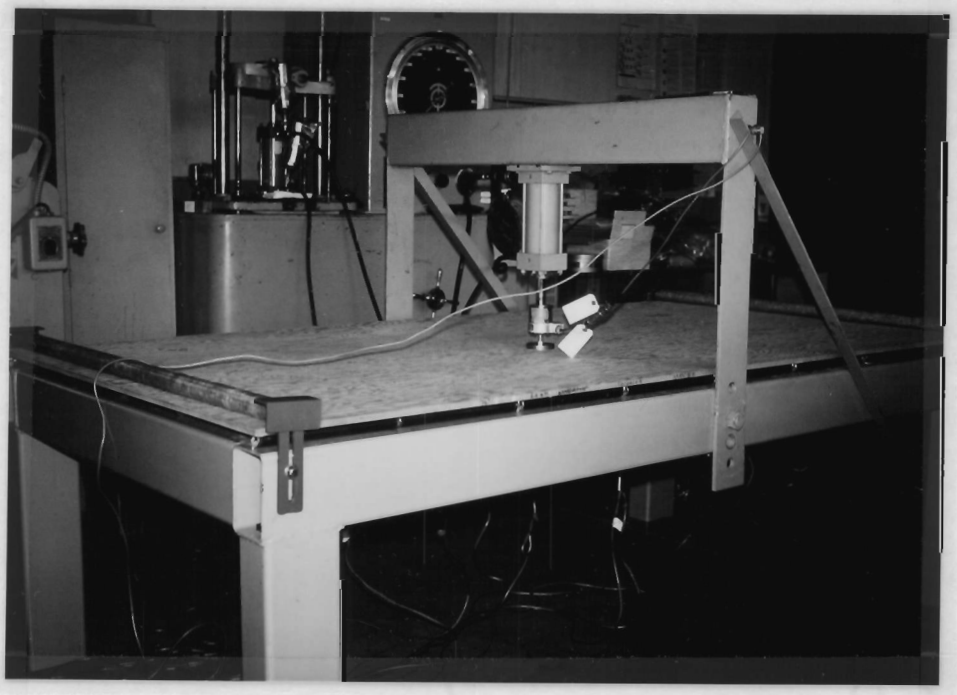

Figure 4.1. Mounted plywood sheet ready for testing.

The deflection was measured by Linear Variable Differential Transformer (LVDT), held in position by two adjustable crossed steel pipes (Figure 4.2), which enabled the positioning of each LVDT to any desired location on the plate.

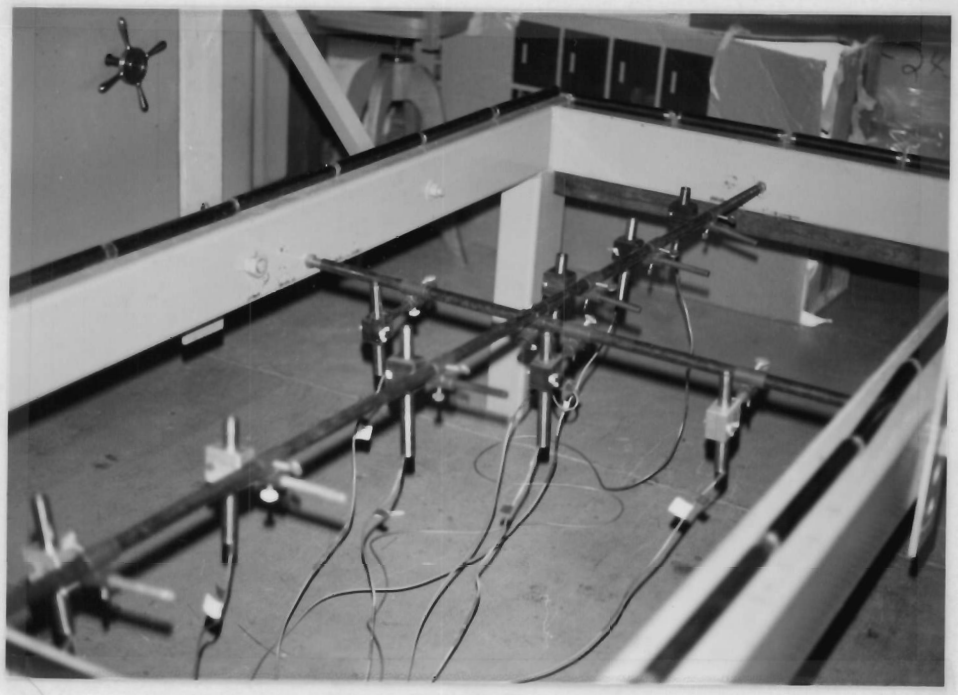

Figure 4.2. LVDT arrangement.

The LVDT is an electro-mechanical device, which produces voltage that is proportional to the displacement of its magnetic core. In this study, the core was suspended by a string from an eye-hook which was attached to the plywood panel, thereby the core could move freely in the LVDT coils. Thus, the LVDT monitored displacements at predetermined positions on the panel (Figure 4.3) continuously as

the board was gradually applied. LVDT's for positions 1, 6 and 7 (Figure 4.3) had two-inch and the remaining LVDT's had one-inch range of linear response.

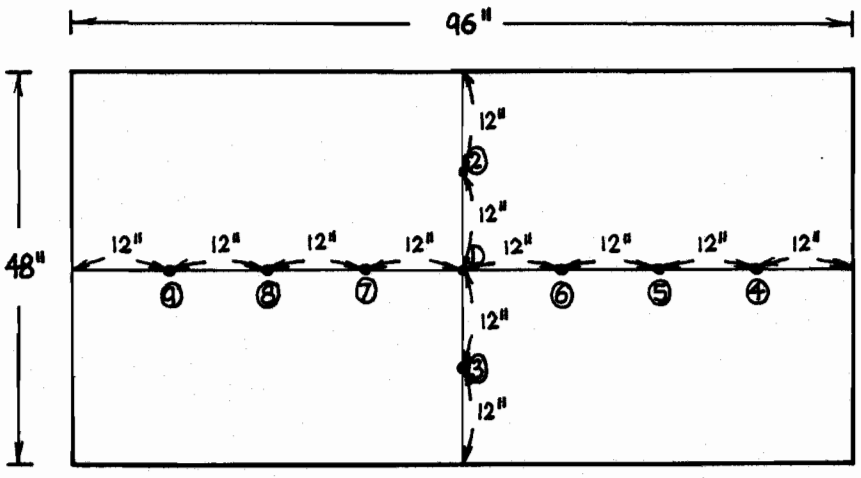

Figure 4.3. Schematic drawing of LVDT arrangement.

The load was monitored continuously by a 1000-pound load cell, an electronic transducer that monitored the applied load with an accuracy of 0.1 pound. Output of the load cell was amplified and recorded by a Hewlett Packard data acquisition system (HP 70043).

A scanner, controlled by a program (Appendix B) executed on the HP 9825A calculator, enabled automatic scanning of LVDT's and load cell at predetermined load increments.

4.2.2. Testing Procedure

Each full sheet was tested twice, once with face veneer upwards and once with face veneer downwards.

Because this study considers plywood to be a two-dimensional system, the testing speed recommended by the ASTM standard which is based on one-dimensional system, do not apply directly. Testing speed that corresponded to the ASTM standard was determined as described in the following paragraph.

The stress-strain equations for simply supported rectangular plate are (17):

$$E_{x}(\frac{a}{2},\frac{b}{2}) = \frac{h}{1 - \nu_{xy}\nu_{yx}} [W,_{xx}(\frac{a}{2},\frac{b}{2}) + \nu_{xy}W,_{yy}(\frac{a}{2},\frac{b}{2})] \qquad (4.1)$$

$$E_{y}(\frac{a}{2},\frac{b}{2}) = \frac{h}{1 - \nu_{xy}\nu_{yx}} [W,_{yy}(\frac{a}{2},\frac{b}{2}) + \nu_{yx}W,_{xx}(\frac{a}{2},\frac{b}{2})] \qquad (4.2)$$

in which $W,_{xx}$ and $W,_{yy}$ represent the curvature of deflection surface W(x,y) along x or y axis, and other symbols have been defined earlier in the text. The speed of testing $\Delta W(x,y)$ equals the deflection rate, which can be calculated by solving either Equation 4.1 or Equation 4.2. Because the E_x is usually larger than E_y, $E_{x}(\frac{a}{2},\frac{b}{2})$ was considered to be the critical strain rate for outerfibers. Thus a computer program (Appendix C) was prepared to numerically solve Equation 4.1 for $\Delta W(x,y)$. For strain rate of beams, ASTM D 3043-76 (1) calls for the rate of 0.0015 in./in. per minute, which is too fast for the maximum scanning rate of the data acquisition system

employed in this study. To permit almost simultaneous scanning of all the points monitored (Figure 4.3), the strain rate of 0.0001 in./in. per minute was chosen. Based on this strain rate, the testing speeds for 3/8-inch, 1/2-inch and 3/4-inch plywood were 0.04 in./min., 0.03 in./min. and 0.02 in./min. respectively.

Throughout the full-sheet test, the recorded data, displacement in inches and load in pounds, were temporarily stored on a cassette tape. Using the stored data, the load-displacement curves for all of the nine LVDT's can be plotted on a same sheet. This is done by initiating a HP 9825A plotter through a program (Appendix D).

4.3. Testing of Plywood Sheet Under Pure Moment

Term "pure moment test" refers to testing of full or half plywood sheets as described in this section.

ASTM standard D 3073-76 (1) specifies a testing machine, which applies uniform moments to the two opposite ends of four- by eight-foot (full sheet) or four- by four-foot (half sheet) plywood sheet. Because such a machine was not available for this study, a modified test was devised to simulate this ASTM panel test.

4.3.1. Testing Arrangement

Tested sheets were simply supported along the two opposite ends and the other two ends were free (Figure 4.4A). The supports consisted of a 50-inch long angle iron and a 50-inch long steel pipe, which were placed onto the top of apparatus shown in Figure 4.1. Loading consisted of six weights suspended from panel edges parallel

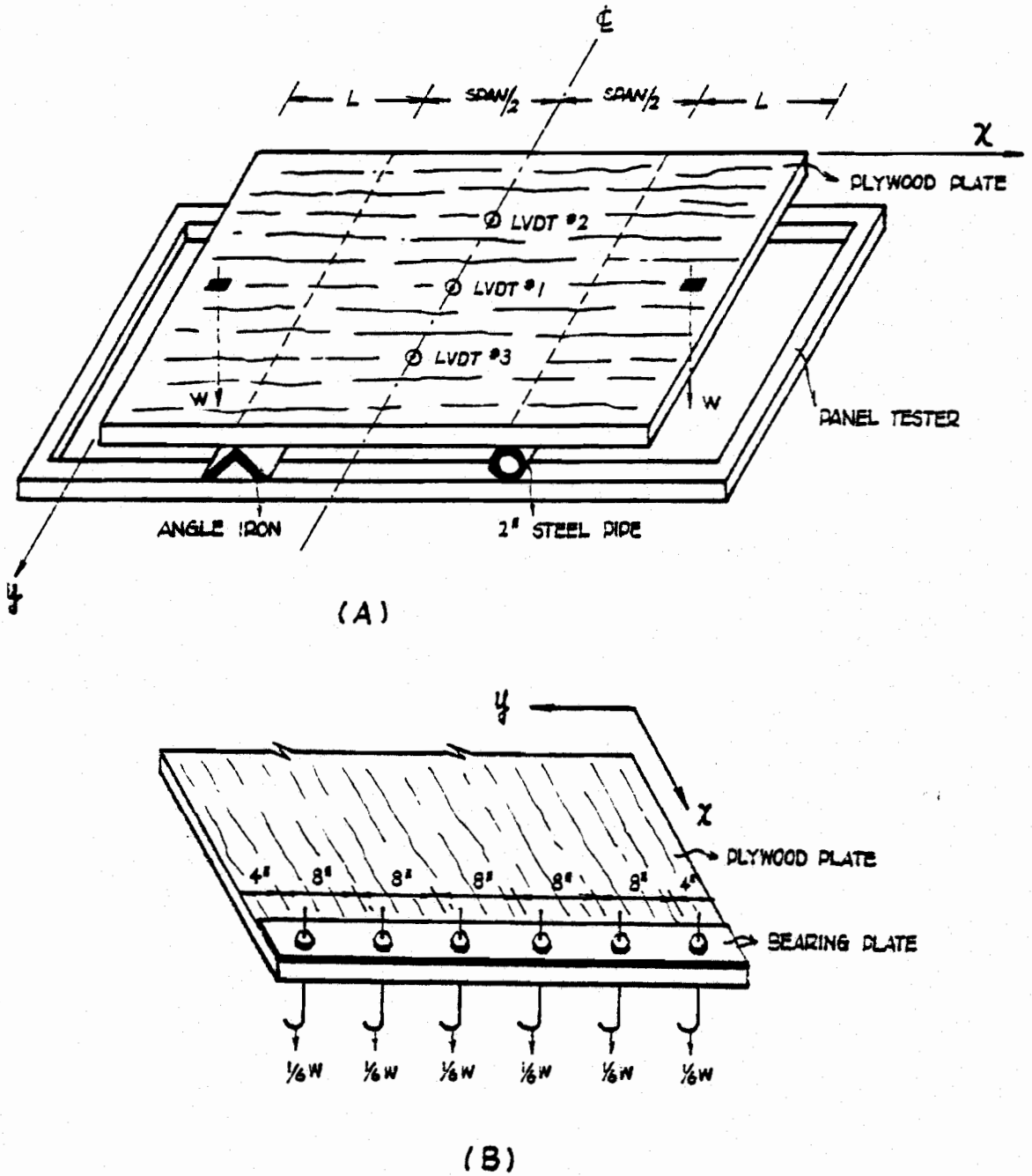

Figure 4.4 (A) Schematic drawing of pure moment test.

(B) Side view of the strip load arrangement.

to supports. To distribute this loading evenly, the weights were attached to the bearing plates that were placed on top of the panel (Figure 4.4B). The external moments on the plate over supports were calculated by multiplying the weights by the overhang width.

As shown in Figure 4.4A, three LVDT's were used to monitor the deflection along the center line. The deflection data was acquired by the system used for full-sheet test.

4.3.2. Testing Procedure

Plywood sheets used for full-sheet tests were used in pure moment tests. Each sheet was tested first uncut with the surface grain parallel to the x-direction (Figure 4.4A). Then, this full sheet was cut into two half-sheets which were tested with surface grain parallel to the y-direction (Figure 4.4A). Each full sheet and each half sheet was tested twice: once with face veneer upwards and once with face veneer downwards.

The weights were applied in two load increments (Table 4.1). The load in the first load increment assured the full contact between the plate and the supports. The second increment provided the deflection measurement for the MOE calculation. Thus deflection is recorded as the net difference between the deflection of the first increment and that of the second increment. The testing conditions are tabulated in Table 4.1.

TABLE 4.1. WEIGHTS, SPAN AND OVERHANG VALUES FOR PURE MOMENT TEST

Thickness (in.)	Weight (lb) for loading increments 1st	2nd	Full-sheet Span (in.)	Full-sheet Overhang (in.)	Half-sheet Span (in.)	Half-sheet Overhang (in.)
3/8	64	39	76	9	42	2
1/2; marine	64	39	70	12	34	6
3/4	35	149	58	18	24	11

4.4. Testing of Plywood Strip in Bending

Sections 4.2 and 4.3 cover non-destructive testing for predicting the MOE's of large plywood sheets. This section deals with the flextural tests of small, simply supported plywood specimens according to ASTM standard D 3043-76 (1).

4.4.1. Specimen Preparation

Two kinds of specimens were cut from sheets tested according to sections 4.2 and 4.3. The first kind had the face grain oriented parallel to the long axis of the strip (in the x-direction), and aimed at evaluating E_x. The second type had face grain oriented perpendicular to long axis of the strip and conducted to evaluate E_y. Specimens were two inches wide, but their length varied with respect to their thickness. All pieces that contained defects, such as knots and gaps between plies, were discarded. The specimen sizes and number of specimens for each plywood thickness are listed in Table 4.2.

After manufacture the specimens were conditioned in the Standard Room (relative humidity of 50%, temperature 75°F) for about seven days until testing.

TABLE 4.2. SPECIMEN DESCRIPTION FOR PLYWOOD STRIP TEST

Thickness (in.)	Face grain parallel to long axis			Face grain perpendicular to long axis		
	No. of specimens	Length* (in.)	Span (in.)	No. of specimens	Length* (in.)	Span (in.)
3/8	48	20	18	48	11	9
1/2; marine	36	26	24	36	14	12
3/4	22	38	36	32	20	18

*All specimens were two inches wide.

4.4.2. Testing Procedure

Specimens were tested in an Instron testing machine according to the ASTM Standard D 3043-76 (1). The testing conditions are listed in Table 4.3.

TABLE 4.3. TESTING CONDITIONS FOR PLYWOOD STRIP TESTS

Thickness (in.)	Diameter of loading block (in.)	Face grain parallel to long axis		Face grain perpendicular to long axis	
		Head speed (cm/min)	Chart speed (cm/min)	Head speed (cm/min)	Chart speed (cm/min)
3/8	1.25	1	2	0.5	2
1/2; marine	1.5	1	1	0.5	1
3/4	2.25	1	1	0.5	2

Supports under the specimen allowed not only for rotation of beam end in the x,y plane, but also for rotations about the beam axis. This arrangement allows for a uniform application of the concentrated

midspan load in the direction across the width of the test specimen. The test was terminated when sufficient deflection was recorded for computing the elastic MOE. The deflection at midspan was monitored by a deflection transducer and plotted simultaneously against the load on a chart paper.

4.5. Measurement of Specimen Thickness and Moisture Content

Before testing total sheet thickness, thickness of individual plies and moisture content of each sheet were measured. The sheet thickness was measured by ASTM standard D 3043-76 (1) at two points along longer edge. The points were one-fourth of the panel length distant from the panel corners. The measurement accuracy was to the nearest 0.001 inch.

Ply thicknesses are needed to calculate the flextural properties in terms of veneer MOE's. The following procedure was devised to measure ply thicknesses. Lines were drawn perpendicularly to the glue line on the smooth ends of the sheet as shown in Figure 4.5. Length $\overline{EB}$ and $\overline{FC}$ of the glue line, length $\overline{GD}$ of the back and sheet thickness $\overline{AD}$ were measured. Based on similar triangles ABE, ACF and ADG, the veneer thickness $\overline{AB}$, $\overline{BC}$ and $\overline{CD}$ was calculated by:

$$\overline{AB} : \overline{AD} = \overline{EB} : \overline{GD} \tag{4.3}$$

$$\overline{AC} : \overline{AD} = \overline{FC} : \overline{GD} \tag{4.4}$$

$$\overline{BC} = \overline{AC} - \overline{AB} \tag{4.5}$$

$$\overline{CD} = \overline{AD} - \overline{AB} - \overline{BC} \tag{4.6}$$

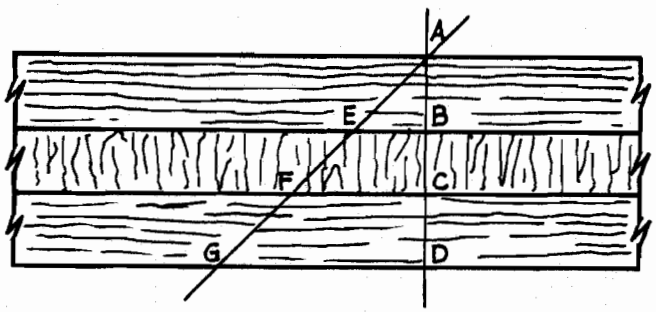

Figure 4.5. Measurement of ply thicknesses.

The moisture content was measured with the capacitance type moisture meter just before testing. Four points were measured on each sheet at locations eight inches from longer edges and two feet distance from the sheet corners.

V. RESULTS AND DISCUSSION

This chapter covers the data analysis procedure, presents the reduced data, and discusses the results of the different tests which were described in Chapter IV.

5.1. Theoretical Evaluation of Average MOE's of Experimental Plywood Panels

The flextural properties of plywood can be estimated from the properties of component plies and of plywood construction by conventional techniques of mechanics of materials (6). The governing equation is:

$$EI = \sum_{i=1}^{n} E_i I_i \tag{5.1}$$

in which

E = effective MOE of plywood;

I = the moment of inertia of the entire cross section about the neutral axis;

E_i = MOE of the i-th ply; and

I_i = the moment of inertia of the i-th ply about the neutral axis of the plywood.

The panels used in this study have plies of various thicknesses so that the neutral axis is not at the midheight of the panel thickness. To locate the neutral axis, it is necessary to know the thickness of individual plies and of the whole panel. The calculation usually used is based on "transformed section," in which the

cross section consisting of more than one material property, is transformed into an equivalent cross section composed of only one material (21). For instance, a three-ply panel with face grain oriented lengthwise (Figure 5.1) is assumed to consist entirely of E_T. The size of the middle ply remains unchanged, but the face and the back ply have their width multiplied by the ratio of longitudinal and tangential MOE: $n = E_L/E_T$. A reasonable value for n of Douglas-fir wood is 20 (6) with average E_L = 1950 Ksi and E_T = 97.5 Ksi.

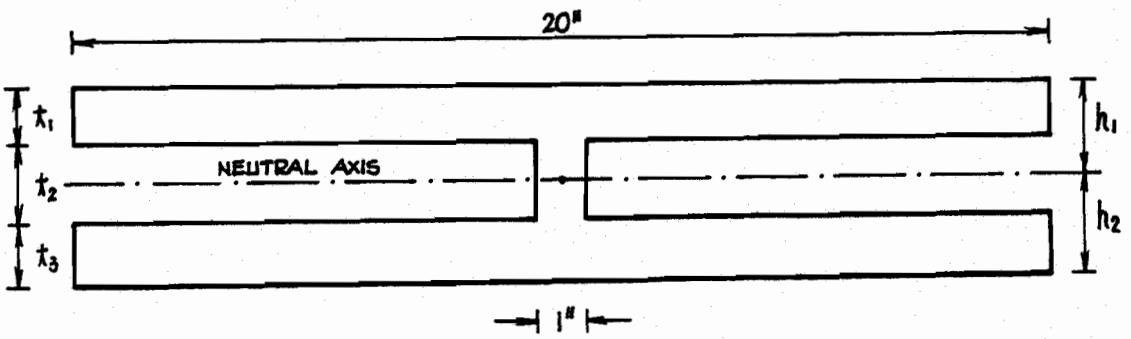

Figure 5.1. Transformed section for calculating effective MOE of plywood panel.

Once the h_1 and h_2 are known, the effective MOE of the plywood panel is calculated in the same way as for the solid I beam. Table 5.1 summarizes the measured properties of experimental panels and computed E_x and E_y based on E_L = 1950 Ksi and n = 20. Because E_L of 1950 Ksi represents average value of clear Douglas-fir solid wood, E_x and E_y in Table 5.1 are the average values of panels of the same configuration as those used in testing.

TABLE 5.1. RESULT OF THEORETICAL EVALUATION.

Panel No.	Panel thickness (in.)	Thickness of ply no. (in.)					h_1 (in.)	MOE of panel (Ksi)	
		1	2	3	4	5		E_x	E_y
1	0.369	0.091	0.179	0.099			0.188	1734	308.8
2	0.360	0.0995	0.175	0.0855			0.174	1717	309
3	0.453	0.090	0.093	0.090	0.090	0.090	0.226	1564	482
4	0.458	0.106	0.095	0.092	0.092	0.073	0.219	1520	500
5	0.731	0.106	0.188	0.156	0.188	0.0938	0.359	1233	779.3
6	0.732	0.079	0.191	0.176	0.199	0.087	0.368	1119	927.8
7	0.475	0.078	0.0899	0.155	0.083	0.0695	0.238	1406	639.9
8	0.487	0.0753	0.0753	0.171	0.0817	0.0837	0.244	1461	580.4

5.2. Experimental Results

5.2.1. Full-size Panels With Simply Supported Edges

Load-displacement curves for eight experimental panels with face veneer upwards are shown in Appendix E. Curves for panels with face veneer downwards are similar, and are omitted. However, both of the curves were used in predicting MOE's. The number above each curve represents the LVDT's position corresponding to Figure 4.3. In most cases, in-plane membrane forces normal to panel edges caused an increased stiffness, when the deflection exceeded half of the panel thickness, t. This observation agrees with that noted by McGleen et al. for square plywood plates (17). These researchers concluded that the membrane forces in simply supported plates got larger as the deflection increased and that the membrane forces became significant when the maximum deflection became greater than t/2. Thus, for the same deflection, the membrane stiffening effects are smaller for larger panel thickness, as indicated by accompanying figures in Appendix E.

As expected, symmetrical points on the panel deflected about the same (Appendix E). For instance, positions (Figure 4.3) 4 and 9; 5 and 8; 3 and 2; 7 and 6 displayed about the same deflection, especially for the initial slope region. However, some variations did occur because of local stiffness variations and defects in plywood panels.

5.2.2. MOE's from Testing of Full-size Panels With Simply Supported Edges

This section deals with the analysis of data from testing described in Section 4.2, which was performed by applying the procedure of Section 3.2.3. This section then presents the predicted values of MOE for directions along and the directions across the face grain.

Before digitizing experimental load-displacement curves of Appendix E, each nonlinear curve was divided into three linear slope regions according to panel thicknesses (Table 5.2).

TABLE 5.2. SLOPE REGIONS USED IN DIGITIZING INELASTIC LOAD DEFLECTION TRACES

Thickness (in.)	Slope region (lb.)		
	1	2	3
3/8	0 - 20	20 - 60	over 60
1/2; marine	0 - 50	50 - 150	over 150
3/4	0 - 200	200 - 500	over 500

Each linear section had a secant modulus which contained the bending and membrane stiffness. However, the initial region, associated with tangent through the coordinate origin, was assumed to define the bending stiffness only. Using the slope of 2nd or 3rd region would tend to overestimate the bending MOE by about 20% because of membrane effects as shown by a primary trial data evaluation of a 1/2-inch plywood panel. Table 5.3 presents the digitized data of loads and displacements. For better estimation of the average

deflection, the deflection for symmetrical points 2,3; 6,7; 5,8; and 4,9 (Figure 4.3) were averaged. The symbol A and/or B in the panel number of Table 5.3 denotes panel tested with face veneer on the top and/or on the bottom.

TABLE 5.3. DIGITIZED LOAD-DEFLECTION DATA FOR INITIAL TANGENT MODULUS.

Panel no.	Load (lbs)	Deflection at points (Figure 4.3)				
		1	(2,3)	(6,7)	(5,8)	(4,9)
1A	10	0.183	0.111	0.152	0.105	0.051
1B	10	0.195	0.118	0.163	0.112	0.054
2A	10	0.218	0.133	0.182	0.126	0.060
2B	10	0.215	0.129	0.180	0.123	0.059
3A	40	0.285	0.157	0.225	0.148	0.067
3B	40	0.283	0.160	0.223	0.147	0.0684
4A	40	0.343	0.195	0.275	0.182	0.083
4B	40	0.342	0.194	0.274	0.172	0.086
5A	200	0.327	0.182	0.248	0.150	0.067
5B	200	0.316	0.171	0.236	0.142	0.065
6A	200	0.327	0.192	0.269	0.147	0.066
6B	200	0.320	0.180	0.240	0.142	0.044
7A	40	0.270	0.147	0.212	0.135	0.060
7B	40	0.264	0.144	0.207	0.128	0.059
8A	40	0.246	0.139	0.208	0.130	0.0604
8B	40	0.242	0.138	0.203	0.125	0.0608

To invert Equation 3.31 by Newton's method of tangents, a set of initial value for E_x and R was needed to initiate the iteration. Because some values of E_x and R may cause divergence or convergence to wrong roots, the effect of initial values of E_x and R on predicted

MOE was studied on a 1/2-inch plywood panel. The results (Table 5.4) showed the effect was minimal. The study also showed that the better the initial estimates the faster the convergence. Therefore, the values in Table 5.1 were used as initial values.

TABLE 5.4. EFFECT OF INITIAL E_x AND R ON PREDICTED MOE.

Input		Output	
E_x (Ksi)	R	E_x (Ksi)	E_y (Ksi)
3000	5.62	764.8	418.8
1000	5.62	764.8	418.9
500	5.62	764.8	418.9
50	2.0	764.6	419.0
50	1.0	759.2	418.9
50	0.3	759.2	419.0

As mentioned in Section 3.2.3, the deflection at two different points is needed to determine a pair of E_x and R. The largest deflection at the center was one of the deflections chosen. The other one is the mean deflection for symmetric locations 2,3; 6,7; 5,8; and 4,9 (Figure 4.3). Trial computations with deflections other than the one at the centroid resulted in arithmetic overflow possibly because of divisions by a very small number. Also, the deflection at the centroid is the best one to use, because it is the largest and, therefore, the most accurately measured.

The results of this data analysis are E_x and E_y ($E_y = RE_x$) of the tested panels (Table 5.5).

TABLE 5.5. COMPUTED E_x AND E_y FROM TESTED DATA ON FULL-SIZE PANELS WITH SIMPLY SUPPORTED EDGES.

Panel no.	Thickness (in.) M.C. (%)	MOE	MOE from deflection at points (2,3)	(6,7)	(5,8)	(4,9)	Face average	Panel MOE	Panel average
1A	0.369	E_x	1474.4	1386.5	1516.5	1341.5	1429.7	E_x	1391.7
		E_y	352.7	357	350	360	354.9		
1B	7.8	E_x	1349.2	1413.4	1441.5	1210.9	1353.7	E_y	341.2
		E_y	325.9	322.7	327.6	333.6	327.5		
2A	0.360	E_x	1277.5	1309.6	1445.3	1127.2	1289.9	E_x	1270.6
		E_y	311.6	311.8	302.4	319.3	311.3		
2B	7.8	E_x	1136.7	1389.7	1346.9	1131.7	1251.3	E_y	315.4
		E_y	325.7	312.3	314	326	319.5		
3A	0.453	E_x	1186.6	1183.9	1256	1032	1164.6	E_x	1189.8
		E_y	467.2	466.1	463.2	469.8	466.6		
3B	7.2	E_x	1280.0	1179.5	1267.7	1132.6	1215	E_y	468.2
		E_y	467.8	471.2	467.5	472.7	469.8		
4A	0.458	E_x	927.2	1041	1061.8	893.3	980	E_x	980.6
		E_y	441.5	435.6	435.2	442.2	438.6		
4B	7.7	E_x	925.1	1041	1061.8	893.3	980.3	E_y	438.8
		E_y	442.6	435.6	435.2	442.2	438.9		
5A	0.731	E_x	954.4	740.1	776.5	891.9	840.7	E_x	811
		E_y	604.1	601.7	601.9	602.7	602.6		
5B	6.1	E_x	794.9	776.0	709.8	844.3	781.3	E_y	614.4
		E_y	625.9	625.8	622.6	630.1	626.1		
6A	0.732	E_x	723.2	658	723.2	723.2	706.9	E_x	715.5
		E_y	597.8	592.8	597.8	597.8	596.6		
6B	6.1	E_x	741.7	741.7	671.1	741.7	724.1	E_y	604.5
		E_y	613	613	610.1	613	612.3		
7A	0.475	E_x	907.6	1020.1	924.3	801.2	913.3	E_x	903.3
		E_y	521.6	517.8	519.3	520.2	519.7		
7B	6.5	E_x	935.2	981.7	821.9	834.3	893.2	E_y	534.8
		E_y	534.4	594	537.2	534	549.9		

TABLE 5.5, Continued:

Panel no.	Thickness (in.) M.C. (%)	MOE	MOE from deflection at points (2,3)	(6,7)	(5,8)	(4,9)	Face average	Panel MOE	Panel average
8A	0.487	E_x	1103.5	1306.6	1254	1086.9	1187.8	E_x	1216.4
		E_y	525.5	518.5	520	527.6	522.9		
8B	6.5	E_x	1331.9	1306.6	1254	1086.9	1244.9	E_y	523.3
		E_y	528.5	518.5	520	527.6	523.7		

The column denoted in Table 5.5 as face average contains the average MOE's from tests of each face, and the column denoted as panel average contains the average MOE's for each panel. Local MOE's on the panel shown in columns 4 through 7 differ less than the local MOE's on piece of lumber, because the defects in plies are randomly distributed throughout the panel. The local MOE on the panel is the combined local MOE for all the plies of the location.

The MOE estimated by this method is based on actual testing and on Equation 3.31 which represents the conditions of testing. Therefore, the E_x and/or E_y are the MOE's which truly represent the panel elasticity along the eight-foot direction and/or along the four-foot direction. Comparing calculated mean MOE values in Table 5.1 to the values from full-sheet tests in Table 5.5 shows that the latter are smaller than the former. Because this comparison is between means and individual observations, the only possible conclusion is that the tested panels were generally weaker than the populations' means.

In summary, the full-sheet testing has the following advantages:

1) It is a full-sheet test resulting in representative E_x and E_y for the panel;
2) It is a non-destructive test; panel can still be utilized after testing;
3) It is time-efficient test; no manufacturing of specimens is needed; and
4) From only one test, E_x and E_y can be estimated simultaneously.

5.2.3. Testing Panel With Opposite Ends Simply Supported and Applied Moments

The purpose of this test was to simulate the ASTM-D 3043 testing method (1). Experimental data from this test was evaluated according to two procedures. The first one is based on the simple beam theory according to the ASTM. The second one calls for evaluation of MOE's from Equation 3.49 in which the panel is treated as a plate.

According to the ASTM, the panel stiffness is derived from the definition of curvature (1):

$$EI = M\rho \tag{5.2}$$

in which

EI = panel bending stiffness in which the moment of inertia, I, is based on the entire cross section;

M = applied bending moment; and

ρ = radius of curvature for deformed plate assumed to act as beam.

Figure 5.2 depicts a simply supported beam subjected to external moments, M. The undeformed beam is represented by a dotted line.

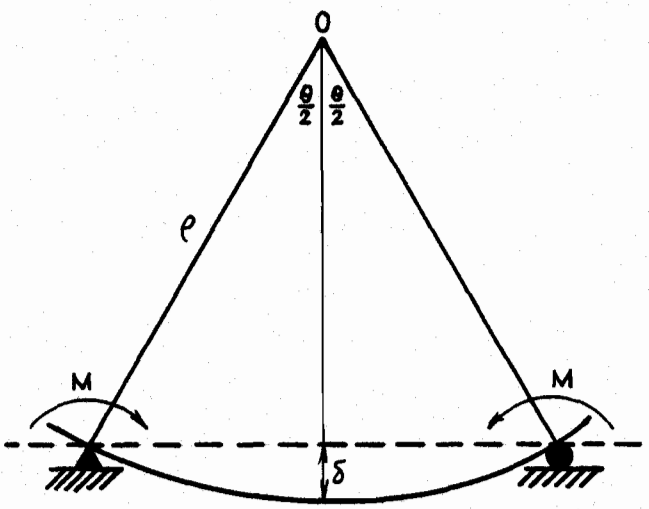

Figure 5.2. Deformation of plate acting as a beam under external support moments.

The radius follows directly from geometry:

$$\rho \cos \frac{\theta}{2} + \delta = \rho \tag{5.3}$$

where

$$\cos \frac{\theta}{2} = \sqrt{\rho^2 - L^2/4} \,/\, \rho$$

Thus,

$$\delta = \rho - \sqrt{\rho - L^2/4} \tag{5.4}$$

from which:

$$\rho = L^2/8\delta + \delta/2 \tag{5.5}$$

Applying Equation 5.2 and Equation 5.5 to experimental data resulted in MOE's shown in Table 5.6.

TABLE 5.6. MOE's FROM PURE MOMENT TEST BASED ON SIMPLE BEAM THEORY

Panel no.	I ($in.^4$)	Full sheet δ (in.)	Full sheet E_x (Ksi)	Half sheet δ (in.)	Half sheet E_y (Ksi)	MOE	Face average	MOE	Panel average
1A	0.201	0.712	1903.3	0.477	193.1	E_x	1903.3	E_x	1853.5
				0.417	220.7	E_y	206.9		
1B		0.752	1804.8	0.474	194	E_x	1804.8	E_y	208.4
				0.408	225.7	E_y	209.9		
2A	0.187	0.774	1629.3	0.430	199.1	E_x	1629.3	E_x	1627.6
				0.423	202.2	E_y	200.6		
2B		0.776	1625.8	0.429	199.5	E_x	1625.8	E_y	195.4
				0.473	180.8	E_y	190.2		
3A	0.372	0.552	1396.4	0.193	471.1	E_x	1396.4	E_x	1407.8
				0.188	483.7	E_y	477.4		
3B		0.543	1419.1	0.195	461.1	E_x	1419.1	E_y	473
				0.193	471.1	E_y	468.6		
4A	0.385	0.618	1204.6	0.201	437.0	E_x	1204.6	E_x	1197.4
				0.235	373.8	E_y	405.4		
4B		0.626	1190.1	0.205	428.5	E_x	1190.1	E_y	402.5
				0.237	370.8	E_y	400		
5A	1.563	0.155	1218.5	0.106	712.3	E_x	1218.5	E_x	1210.6
				0.093	811.8	E_y	769		
5B		0.157	1202.8	0.105	719.1	E_x	1202.8	E_y	760
				0.097	778.4	E_y	751		
6A	1.569	0.170	1106.9	0.100	752.2	E_x	1106.9	E_x	1106.9
				0.090	835.7	E_y	794		
6B		0.170	1106.9	0.098	767.5	E_x	1106.9	E_y	805
				0.087	864.5	E_y	816		
7A	0.429	0.602	1110.5	0.111	710.2	E_x	1110.5	E_x	1120.9
				0.108	729.8	E_y	720		
7B		0.591	1131.3	0.113	697.6	E_x	1131.3	E_y	720.3
				0.106	743.5	E_y	720.6		

TABLE 5.6, Continued:

Panel no.	I ($in.^4$)	Full sheet δ (in.)	Full sheet E_x (Ksi)	Half sheet δ (in.)	Half sheet E_y (Ksi)	MOE	Face average	MOE	Panel average
8A	0.462	0.360	1724.1	0.108	677.7	E_x	1724.1	E_x	1717
				0.126	580.9	E_y	629.3		
8B		0.363	1709.9	0.108	677.7	E_x	1709.9	E_y	630.5
				0.125	585.5	E_y	631.6		

The MOE's in Table 5.6 are much higher than the MOE's for the full-sheet test (Table 5.5). This difference is the highest for E_x. (An exception is E_y for the 3/8-inch plywood, which is smaller than the E_y in Table 5.5.) The main reason for the differences is the error associated with analyzing the plate by beam equation. Another reason is the validity of the beam equation for large deflection; equation $EI = M\rho$ is accurate only if the angles of rotation at supports are very small.

Another method, also used to calculate the MOE's from pure moment test consisted of inverting Equation 3.49. The resulting MOE's were based on deflections and moments from testing and on plate geometry. Trial-and-error technique was used to invert Equation 3.49, in which various values were assumed for MOE's and then the deflections calculated. The assumed MOE with calculated deflection the closest to the experimental deflection was the desired value. Initially assumed values for E_x and E_y were those of Table 5.6. Then the values for E_x and E_y of Table 5.6 were increased and decreased by multiples of 20 Ksi and the deflection calculated. The procedure was repeated until the computed deflection agreed with the corresponding experimental deflection. Program PMTMOE (Appendix F) was prepared to perform these computations; Table 5.7 depicts the resulting MOE's.

TABLE 5.7. MOE's EVALUATED ACCORDING TO PLATE THEORY

Panel no.	Thickness (in.)	E_x (Ksi)	E_y (Ksi)
1	0.369	1510	230
2	0.360	1450	220

TABLE 5.7, Continued:

Panel no.	Thickness (in.)	E_x (Ksi)	E_y (Ksi)
3	0.453	1210	480
4	0.458	1020	420
5	0.731	890	670
6	0.732	870	610
7	0.475	900	550
8	0.487	1300	570

Comparison between the MOE's in Table 5.6 and in Table 5.7 suggests that MOE's based on simple beam theory are higher by about 10% to 25%, because this theory neglects the two-way action of a plate. The MOE's evaluated according to the plate theory by Equation 3.49 (Table 5.7) were close to those based on the full-sheet tests (Table 5.5).

Additional disadvantages of the ASTM method for evaluating MOE's of plywood are:

1) Error in MOE may be also caused by deflection measurement; the deflection at the plate centroid does not always represent the average deflection across the whole plate width; and
2) A separate test has to be conducted to get MOE in each direction of the sheet; full sheet is usually tested to get MOE along the eight-foot direction and half sheet is tested subsequently to get MOE along the four-foot direction of the sheet.

5.2.4. Bending Tests of Plywood Strips

For bending tests, specimen stiffness was calculated by the following equation:

$$EI = (L^3/48)\ (P/\delta) \tag{5.6}$$

in which

EI = bending stiffness in which the moment of inertia I was based on the entire cross section;

P/δ = slope of the load-deflection curve within the elastic range; and

L = span length.

The load-deflection curves were recorded in kilograms and centimeters, respectively. The observed data was digitized and converted into pounds and inches, then inserted in Equation 5.6 to compute MOE's statistically. Reduced data are shown in Table 5.8.

TABLE 5.8. MOE's FROM BENDING TESTS OF PLYWOOD STRIPS

Test no.	No. of specimens	I ($in.^4$)	E_x (Ksi)	Std. dev. (Ksi)	E_y (Ksi)	Std. dev. (Ksi)	Average	
1A	48	8.37×10^{-3}	1489.7	279.3	194.4	54.8	E_x	1555
1B			1620.2	260.7	170.2	38.3	E_y	182.3
2A	48	7.78×10^{-3}	1297.8	212.7	179.2	38.6	E_x	1406
2B			1514.1	199.6	181.5	96.2	E_y	180.4
3A	36	15.5×10^{-3}	1385.1	133.9	484.1	159.7	E_x	1343
3B			1301.0	175.7	330.8	164.7	E_y	407.5
4A	36	16.0×10^{-3}	1318.6	119.9	417.5	80.9	E_x	1262.2
4B			1205.8	148.7	398.6	95.0	E_y	408.1
5A	E_x:22	65.1×10^{-3}	1039.7	99.2	663.9	119.0	E_x	1007.7
5B	E_y:32		975.6	168.9	647.9	118.5	E_y	655.6
6A	E_x:22	65.4×10^{-3}	825.7	146.2	684.1	95.9	E_x	809.3
6B	E_y:32		792.8	79.6	703.9	91.8	E_y	694
7A	36	17.9×10^{-3}	1076.9	100.2	643.2	61.0	E_x	1076.9
7B			1125.8	119.7	601.8	33.9	E_y	622.5
8A	36	19.3×10^{-3}	1570.4	80.6	578.5	86	E_x	1545
8B			1519.6	111.0	587.1	99.8	E_y	582.8

Standard deviation for the calculated MOE's varies between 100 Ksi and 200 Ksi. Higher-grade of plywood should display smaller variability than lower-grade panels, because the former had smaller intra-panel variations in local MOE's. The advantage of this method is the simplicity in the evaluation of test data that is enabled by the simple beam equation which simulates the testing condition. However, to get the accurate estimate of the mean MOE for the panel, enough specimens should be tested. In this study, the MOE's are 10% to 20% higher than those of the full-sheet test (Table 5.9). Possible reason for higher MOE's is the gaps and knots contained in full sheet but not in strips. (Strips with gaps between plies were discarded.) Also in Table 5.9, individual MOE for the ASTM test was compared to the corresponding MOE of the plywood strip test by the "% difference."

The main disadvantages of this test are:

1) Each strip test evaluates only the MOE in one direction;
2) Making test specimens is time consuming and results in destroying the plywood panel, also specimens with knots and gaps are not suitable for testing; and
3) Each test gives a local MOE on the panel and many tests are needed to determine the average MOE of the panel.

TABLE 5.9. MOE DIFFERENCE BETWEEN PLYWOOD STRIP TEST AND INDICATED TEST

Panel no.	MOE	MOE Plywood strip (Ksi)	Full-sheet test (%)	ASTM test (%) (Beam theory)	ASTM test (%) (Plate theory)
1	E_x	1555	-10.5	+19.2	- 2.9
	E_y	182.3	+87.2	+14.3	+26.2
2	E_x	1406	- 9.6	+15.8	+ 3.1
	E_y	180.4	+74.8	+ 8.3	+22
3	E_x	1343	-11.4	+ 4.8	- 9.9
	E_y	407.5	+14.9	+16.1	+17.8
4	E_x	1262.2	-28.8	- 4.1	-19.2
	E_y	408.1	+ 7.5	- 0.1	+ 2.9
5	E_x	1007.7	-19.5	+20.1	-11.7
	E_y	655.6	- 6.2	+15.9	+ 2.2
6	E_x	809.3	-11.6	+36.7	+ 7.5
	E_y	694	-12.9	+16	-12.1
7	E_x	1076.9	-16.1	+ 4	-16.4
	E_y	622.5	-14.1	+15.7	-11.6
8	E_x	1545	-21.3	+11.1	-15.9
	E_y	582.8	-10.2	+ 7.6	- 2.2

VI. CONCLUSIONS AND RECOMMENDATIONS

The investigation described in this thesis resulted in the following conclusions:

1) A procedure, based on testing full-size plywood panels, simply supported on edges, correctly predicts representative E_x and E_y for the panel. The MOE's according to this method are accurate, because they are computed from experimental deflections by equation followed the theory that truly represents testing conditions;
2) The MOE's from the ASTM test differed from those of the full-sheet test by about 20% to 35%, mainly because the ASTM test neglects the two-way action and because of within-the-panel stiffness variation (this difference was not confirmed statistically);
3) Applying an appropriate plate equation to evaluate MOE's from the ASTM tests resulted in MOE's that are close to those of the full-sheet test;
4) Testing of plywood strip bending results in accurate MOE, assuming that the strips represent all the local properties on the panel;
5) Testing of full-size simply supported plywood panel does not destroy the panel which can subsequently be used for other purposes; and
6) Making specimens for plywood strip testing is time consuming and results in destroying the plywood panel.

The following are recommendations of this study:

1) Because only eight plywood sheets are tested to evaluate stiffness properties, this study may lack significance for statistical comparison of MOE's among the three testing procedures;
2) The use of simply-supported plate tests to evaluate MOE's of panel materials thinner than 3/8-inch may be questionable. A study is needed to explore this use; and
3) The possibility should be investigated of using the full-sheet tests for orthotropic panels other than those of plywood, such as gypsum board and particleboard.

BIBLIOGRAPHY

1. American Society for Testing and Materials. 1977. Annual Book of ASTM Standards - Part 22, Wood, Adhesives. ASTM. Philadelphia, Pa. 1042 pp.

2. Ashton, J. E. and J. M. Whitney. 1970. Theory of Laminated Plates. Progress in Material Science Series Vol. V, Technomic Publication, Conn.

3. Biblis, E. J. 1969. Flextural rigidity of southern pine plywood. Forest Prod. J. 19(6):47-54.

4. Biblis, E. J. and Y. M. Chiu. 1969. An analysis of flextural elastic behavior of three-ply southern pine plywood. Wood and Fiber 1(2):154-161.

5. Bodig, J. and J. R. Goodman. 1973. Prediction of elastic parameters for wood. Wood Science 5(4):249-264.

6. Chiu, Y. M. and E. J. Biblis. 1973. Compression of flextural properties and dimensional stability of two construction of 5/8 inch five-ply southern pine plywood. Agricultural Experiment Station. Auburn University, Auburn, Alabama.

7. Gunnerson, R. A., J. R. Goodman, and J. Bodig. 1973. Plate tests for determination of elastic parameters of wood. Wood Science 5(4):241-248.

8. Hearmon, R. F. S. 1952. The bending and twisting of orthotropic plates. British J. of Applied Physics 3:150-156.

9. Hearmon, R. F. S. 1961. An introduction to applied anisotropic elasticity. Oxford University Press, Oxford. London. 136 pp.

10. Hoppmann, W. H. 2nd. 1955. Bending of orthogonally stiffened plates. J. of Applied Mechanics Trans. ASME Vol. 77. 267-271.

11. Huffington, N. J. 1956. Theoretical determination of rigidity properties of orthogonally stiffened plates. J. of Applied Mechanics 23(1):15-20.

12. Hunt, M. O. and S. K. Suddarth. 1974. Prediction elastic constants of particleboard. Forest Prod. J. 24(5):52-57.

13. Jayne, B. A. and M. O. Hunt. 1969. Plane stress and plane strain in orthotropic and anisotropic media. Wood and Fiber 1(3):236-247.

14. Lee, W. C. and E. J. Biblis. 1977. New approach for determination of elastic constants of orthotropic wood-base plates by strip bending and plate twisting. Wood Science 9(4):160-166.

15. Lekhnitski, S. G. 1968. Anisotropic plates. 2nd Edition. Gordon and Breach, New York.

16. Masuda, M., H. Sasaki and T. Maku. 1968. Numerical analysis of orthotropic plates (1). Wood Research 47(12):12-29.

17. McFarland, D., B. L. Smith, and N. D. Bernhart. Analysis of plates. Spartan Books, New York.

18. McGleen, J. and B. J. Hartz. 1968. Finite element analysis of plywood plates. J. of the Structure Division. Proceedings of the ASCE. 94(ST2):551-563.

19. McLain, T. E. and J. Bodig. 1974. Determination of elastic parameters of full-size wood composite board. Forest Prod. J. 24(14):48-57.

20. Salvadori, M. G. and M. L. Baron. 1961. Numerical methods in engineering. 2nd Edition. Prentice-Hall, Inc. Englewood Cliffs, N.J. 302 pp.

21. Swada, M. and K. Ueda. 1967. Studies on the wooden plates 1. Deflection of rectangular plates under a concentrated load at the center, edges simply supported. Research Bulletin of the College Experiment Forest. Hokkaido University 25(1):61-84.

22. Timoshenko, S. 1940. Theory of plates and shells. McGraw-Hill Book Inc. New York. 580 pp.

23. Timoshenko, S. P. and J. M. Gere. 1972. Mechanics of materials. D. Van Nostrand Company, Canada. 552 pp.

24. Ueda, K. 1968. Studies on the elastic constants of wooden sheet materials. Report 1: The elastic constants of Lauan (Lorea sp.) plywood. Research Bulletin of the College Experiment Forest. Hokkaido Univ. 26(1):143-169.

25. Watanuki, Y., K. Ueda, and H. Okuyama. 1972. Studies on the elastic constants of wooden sheet materials. Report 2: The elastic constants of two-species plywood. Research Bulletin of the College Experiment Forest. Hokkaido Univ. 29(2):335-359.

26. Witt, R. K., W. H. Hoppman 2nd, and R. S. Buxbaum. 1953. Determination of elastic constants of orthotropic material with special reference to laminate. ASTM Bulletin No. 194, pp. 53-57.

27. Wood Handbook. 1974. USDA Agriculture Handbook No. 72. U.S.D.A. Forest Service, Forest Products Lab.

APPENDICES

APPENDIX A

```
      PROGRAM PLYMOE(INPUT,OUTPUT)
C     THIS IS THE PROGRAM BEING USED TO ESTIMATE MOE FOR PLYWOOD
C     PLATE BY GIVING THE VALUES OF:
C     Q:APPLIED LOAD(LB); X1,Y1:X AND Y COORDINATE OF THE 1ST POINT
C     DEFLTN:EXPERIMENTAL DEFLECTION AT(X1,Y1)
C     T:THICKNESS OF THE PLATE(IN)
C     X,Y:X AND Y COORDINATE OF THE 2ND POINT
C     DEFLTN2:EXPERIMENTAL DEFLECTION AT (X,Y)
C     R:RATIO OF THE MOE IN X DIRECTION TO Y DIRECTION
C     EX:MOE IN X DIRECTION (LONG AXIS)
C     G:MODULUS OF RIGIDITY(152.1 KSI FOR D-FIR PLYWOOD)
C     V:POISSON RATIO(0.449 FOR D-FIR PLYWOOD)
C     A,B: PLATE DIMENSION(A=96 IN;B=48 IN )
C
C
C     PROGRAM CODED BY PAUL CHEN (MAY 1980)
C     DETAILED FLOW CHART IS SHOWN IN FIG 3.2 OF THIS ARTICLE
      DIMENSION HP1(5000),HP2(5000),TI1(5000),TI2(5000),PEX(5000)
      READ *,Q,X1,Y1,DEFLTN,T
      READ *,R,EX
      G=152.1E+3
      V=0.449
      A=96.
      B=48.
      I1=0
      KK=0
      PI=3.14159
   10 W=V*V/R
   20 DX=(T**3)*EX/(12*(1-W))
      EY=EX/R
      DY=DX/R
      H=((V*EY)/(1-W)+2*G)*(T**3)/12
      I=0
      FF1=0
      FF2=0
      DO 40 M=1,9,2
      DO 30 N=1,9,2
      I=I+1
      D=(M**4)*DX/(A**4)+2*M*M*N*N*H/(A*A*B*B)+(N**4)*DY/(B**4)
      DE1=(M**4)*(T**3)/(12*(A**4)*(1-W))
      DE2=M*M*N*N*V*(T**3)/(6*A*A*B*B*(R-V*V))
      DE3=(N**3)*(T**3)/(12*(B**4)*(1-W))
      DE=-(DE1+DE2+DE3)
      F1=SIN(M*PI/2)*SIN(N*PI/2)*SIN(M*PI*X1/A)*SIN(N*PI*Y1/B)/D
      F2=SIN(M*PI/2)*SIN(N*PI/2)*SIN(M*PI*X1/A)*SIN(N*PI*Y1/B)*DE/(D**2)
      FF1=F1+FF1
      FF2=F2+FF2
```

APPENDIX A-CONTINUED

```
      HP1(I)=FF1
      HP2(I)=FF2
   30 CONTINUE
      FF1=0
      FF2=0
   40 CONTINUE
      DO 45 I=6,25
      HP1(I)=HP1(I-5)+HP1(I)
      HP2(I)=HP2(I-5)+HP2(I)
   45 CONTINUE
      DEFL1=(4*Q*HP1(25)/(A*B*(PI**4)))-DEFLTN
      DEFL2=4*Q*HP2(25)/(A*B*(PI**4))
      IF(ABS(DEFL1/DEFL2).LE.999) GO TO 50
      EX=EX-DEFL1/DEFL2
      KK=KK+1
      IF(KK.GE.100) GO TO 110
      GO TO 20
   50 I1=I1+1
      PEX(I1)=EX
      IF(I1.EQ.1) GO TO 54
      COMPEX=ABS(PEX(I1)-PEX(I1-1))
      IF(COMPEX.LE.999) GO TO 110
   54 KK=0
      IF (I1.EQ.1) READ *,X,Y,DEFLTN2
      IF (I1.EQ.1) WRITE *,"PREDICTED VALUES OF R AND EX ARE"
   55 W=V*V/R
      DX=(T**3)*EX/(12*(1-W))
      EY=EX/R
      DY=DX/R
      J=0
      GG1=0
      GG2=0
      DO 80 M=1,9,2
      DO 60 N=1,9,2
      J=J+1
      S1=(M**4)*(T**3)*EX/(12*(A**4)*(1-W))
      S2=(M*M*N*N)*(T**3)*V*EX/(6*(A*A*B*B*(R-V*V)))
      S3=(N**4)*(T**3)*EX/(12*(B**4)*(R-V*V))
      S4=M*M*N*N*(T**3)*G/(3*A*A*B*B)
      S=S1+S2+S3+S4
      SE1=-12*(M**4)*(T**3)*V*V*(A**4)*EX/(((12*(A**4)*(1-W))**2)*R*R)
      SE2=-6*(M*M*N*N*(T**3))*V*EX*A*A*B*B/((6*A*A*B*B*(R-V*V))**2)
      SE3=-12*(N**4)*(T**3)*(B**4)*EX/((12*(B**4)*(R-V*V))**2)
      SE=-(SE1+SE2+SE3)
      G1=SIN(M*PI/2)*SIN(N*PI/2)*SIN(M*PI*X/A)*SIN(N*PI*Y/B)/S
      G2=SIN(M*PI/2)*SIN(N*PI/2)*SIN(M*PI*X/A)*SIN(N*PI*Y/B)*SE/(S**2)
```

APPENDIX A-CONTINUED

```
      GG1=G1+GG1
      GG2=G2+GG2
      TI1(J)=GG1
      TI2(J)=GG2
   60 CONTINUE
      GG1=0
      GG2=0
   80 CONTINUE
      DO 90 I=6,25
      TI1(I)=TI1(I-5)+TI1(I)
      TI2(I)=TI2(I-5)+TI2(I)
   90 CONTINUE
      DEFLR1=(4*Q*TI1(25))/(A*B*(PI**4))-DEFLTN2
      DEFLR2=4*Q*TI2(25)/(A*B*(PI**4))
      IF (ABS(DEFLR1/DEFLR2).LE.0.099) GO TO 10
      R=R-DEFLR1/DEFLR2
      KK=KK+1
      IF(KK.GE.100) GO TO 110
      GO TO 55
  110 PRINT *,R,EX
      STOP
      END
 EOI ENCOUNTERED.
/
```

APPENDIX B

```
0: DIM D$[10]
1: ENT "DATE ?",D$
2: ENT "NUMBER OF CHANNELS ?",N
3: ENT "MAXIMUM NUMBER OF SAMPLES",M
4: DIM A$[10],L[M],D[N-1,M],K[N],O[N]
5: D$]A$
6: LDF 4,K[*]
7: "TEST":
8: ENT "TEST NO ?",T
9: PRT "TEST NO",T;PRT "DATE",D$
10: ENT "LOAD INCREMENT BETWEEN SAMPLES ?",R
11: PRT "LOAD INCREMENT",R
12: DSP "PRESS CONTINUE FOR NO LOAD CONDITION";BEEP
13: STP
14: PRT "REFERENCES"
15: FOR I=0 TO N-1
16: FXD 0;PRT "CHANNEL",I
17: CLI 7
18: WTB 2,255-I-6*INT(I/10)
19: WAIT 50
20: RED 722,Z;RED 722,O[I+1]
21: FXD 4;PRT O[I+1]
22: NEXT I;BEEP
23: DSP "PRESS CONTINUE TO START TEST";BEEP;STP
24: 0]P
25: FOR J=1 TO M
26: CLI 7
27: RED 722,Z,"DUMMY READ"
28: WTB 2,255;WAIT 40
29: CLI 7
30: RED 722,A;DSP "LOAD=",(A-O[1])/K[1]]L[J]
31: IF ABS(L[J]-P)<R;JMP -1
32: FOR I=1 TO N-1
33: WTB 2,255-I-6*INT(I/10);WAIT 40
34: CLI 7
35: RED 722,Z;RED 722,B
36: ABS(B-O[I+1])/K[I+1]]D[I,J]
37: NEXT I
38: L[J]]P
39: WTB 2,255;CLI 7;WAIT 40
40: RED 722,Z;RED 722,A
41: ((A-O[1])/K[1]+L[J])/2]L[J];SPC
42: PRT "LOAD (LBS)",L[J]
43: PRT "DISPLACEMENTS";FOR I=1 TO N-1
44: PRT D[I,J];NEXT I
45: NEXT J;BEEP
46: DSP "DATA CASSETTE IN PLACE ?";STP
47: FDF T
48: MRK 1,(N*M+5)*8
49: RCF T,A$,L[*],D[*]
50: PRT "DATA RECORDED ON TAPE"
51: GTO "TEST"
52: END
```

APPENDIX C

```
      PROGRAM LDSPD(INPUT,OUTPUT)
C     THIS IS A PROGRAM TO CALCULATE LOADING SPEED FOR
C     FULL SHEET PLYWOOD WITH DIFFERENT THICKNESS AND MOE
C     SR: RATE OF OUTER FIBER STRAIN,TAKEN AS 0.0001IN/IN.MIN
C     Q: UNIT LOADING,TAKEN AS 1LB
C     WXX:CURVATURE OF DEFLECTION SURFACE W(X,Y) ALONG X AXIS
C     WYY:CURVATURE ALONG Y AXIS
C     PLATE DIMENSION,G,V, ARE THE SAME VALUE AS SPECIFIED IN
C     PROGRAM PLYMOE.
C     PROGRAM CODED BY PAUL CHEN (JUNE 1980)
C
C
      DIMENSION HP(5000),HP1(5000),HP2(5000)
      READ *,EX,R,T
      A=96.
      B=48.
      X=48.
      Y=24.
      G=152.1E+3
      V=0.449
      Q=1.
      SR=0.0001
      PI=3.14159
      W=V*V/R
      DX=(T**3)*EX/(12.*(1-W))
      EY=EX/R
      DY=DX/R
      H=((V*EY)/(1-W)+2*G)*(T**3)/12.
      I=0
      FF=0.
      FF1=FF2=0.
      DO 40 M=1,9,2
      DO 30 N=1,9,2
      I=I+1
      D=((M**4)*DX/(A**4))+(2*M*M*N*N*H/(A*A*B*B),+((N**4)*DY/(B**4))
      F=SIN(M*PI/2)*SIN(N*PI/2)*SIN(M*PI*X/A)*SIN(N*PI*Y/B)/D
```

APPENDIX C-CONTINUED

```
      F1=SIN(M*PI/2)*SIN(N*PI/2)*SIN(M*PI*X/A)*SIN(N*PI*Y/B)*M*M/D
      F2=SIN(M*PI/2)*SIN(N*PI/2)*SIN(M*PI*X/A)*SIN(N*PI*Y/B)*N*N/D
      FF=F+FF
      FF1=F1+FF1
      FF2=F2+FF2
      HP(I)=FF
      HP1(I)=FF1
      HP2(I)=FF2
   30 CONTINUE
      FF=0.
      FF1=FF2=0.
   40 CONTINUE
      DO 45 I=6,25
      HP(I)=HP(I-5)+HP(I)
      HP1(I)=HP1(I-5)+HP1(I)
      HP2(I)=HP2(I-5)+HP2(I)
   45 CONTINUE
      DEFLTN=4*Q*HP(25)/(A*B*(PI**4))
      WXX=4.*Q*HP1(25)/((A**3)*B*(PI**2))
      WYY=4.*Q*HP2(25)/(A*(B**3)*(PI**2))
      SRYY=SR*(1-W)/(((WYY+WXX*V/R)/DEFLTN)*T)
      PRINT *, SRYY
      STOP
      END
 EOI ENCOUNTERED.
/
```

APPENDIX D

```
0: TRK 0
1: ENT "TEST NO ?",T
2: ENT "NUMBER OF CHANNELS ?",N
3: FDF T
4: IDF A,A,A,C
5: (C-40)/(8*N)]M
6: DIM B$[10],L[M],D[N-1,M]
7: LDF T,B$,L[*],D[*]
8: SCL -.3,D[1,M],-100,L[M]
9: AXE 0,0,.1,100
10: CSIZ 2,1.5,.73,0
11: PEN;PLT D[1,M]-.5,100
12: CPLT 0,0
13: LBL "TEST",T
14: FXD 1;0]K
15: "ABCIS":
16: PLT K,0
17: CPLT -2,-1
18: LBL K
19: K+.2]K
20: IF K<D[1,M];GTO "ABCIS"
21: PLT D[1,M]/2,0
22: CPLT -9,-3
23: LBL "DISPLACEMENTS(INCHS)"
24: FXD 0
25: CSIZ 2,1.5,.73,0
26: 0]K
27: "ORD":
28: PLT 0,K
29: CPLT -5,0
30: LBL K
31: K+100]K
32: IF K<L[M];GTO "ORD"
33: PLT 0,L[M]/2
34: CPLT -5,-4
35: CSIZ 2,1.5,.73,90
36: LBL "LOAD(LBS)"
37: "PLOT":
38: BEEP;ENT "LVDT NO ?",R1
39: PEN;PLT 0,0
40: FOR I=1 TO M
41: PLT D[R1,I],L[I]
42: NEXT I;PEN
43: INT(M/2)]J
44: CSIZ 2,1.5,.73,0
45: PLT D[R1,J],L[J]
46: CPLT .2,0
47: LBL R1
48: GTO "PLOT"
49: END
```

APPENDIX E

The following are load-displacement curves for the full-sheet tests:

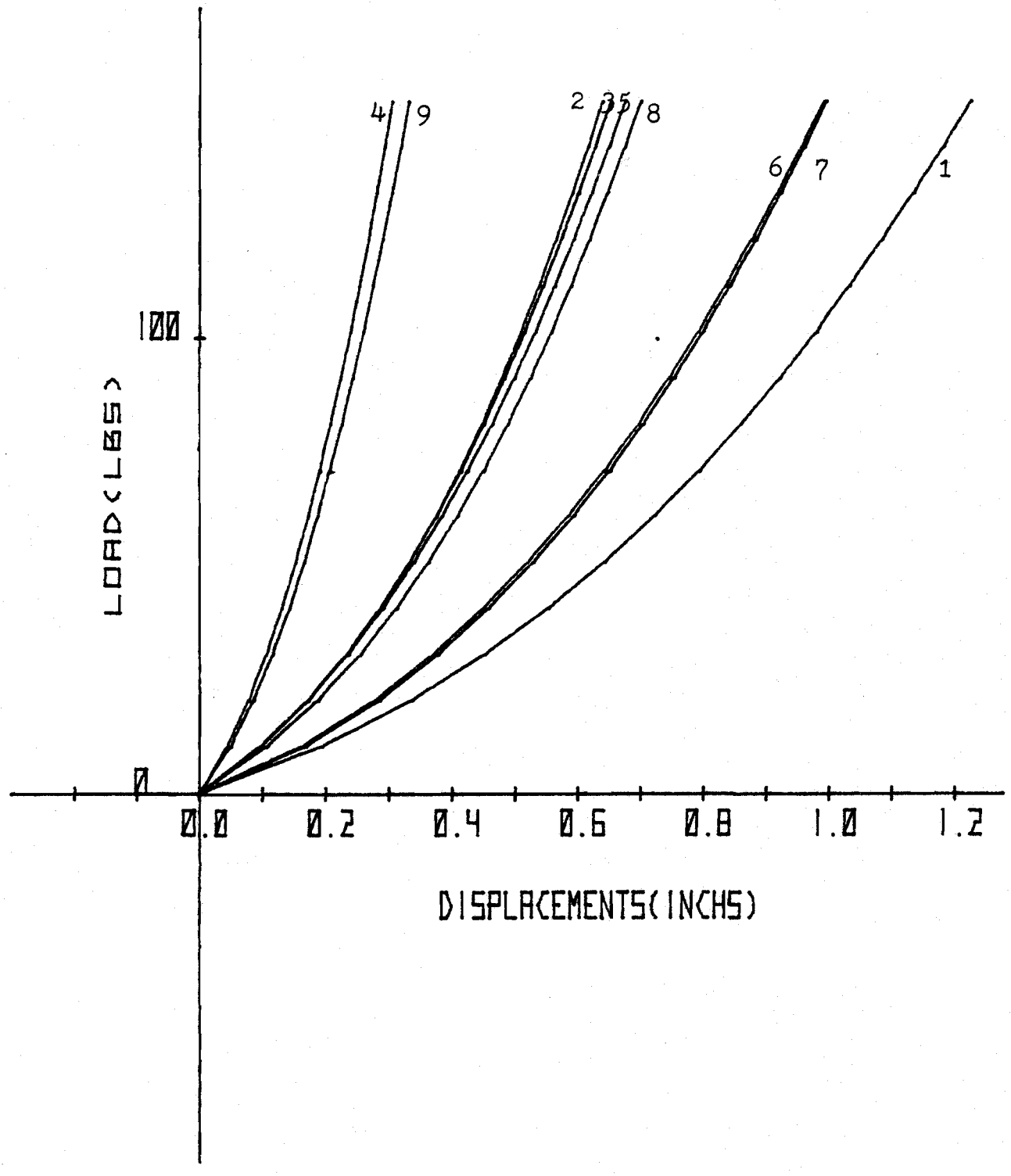

Load-displacement curves of panel no. 1A (t=0.369in.)

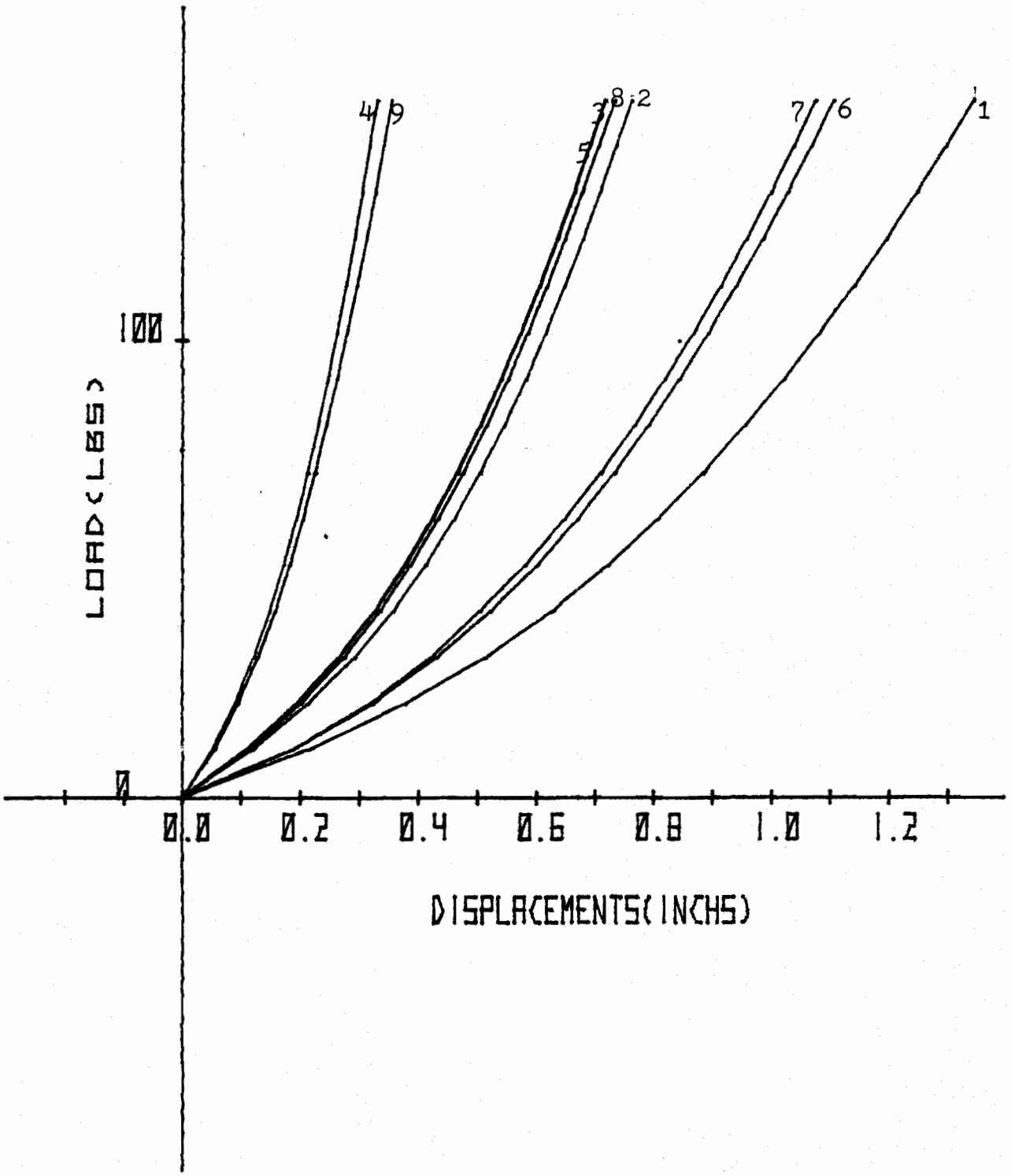

Load-displacement curves of panel no. 2A (t=0.360 in.)

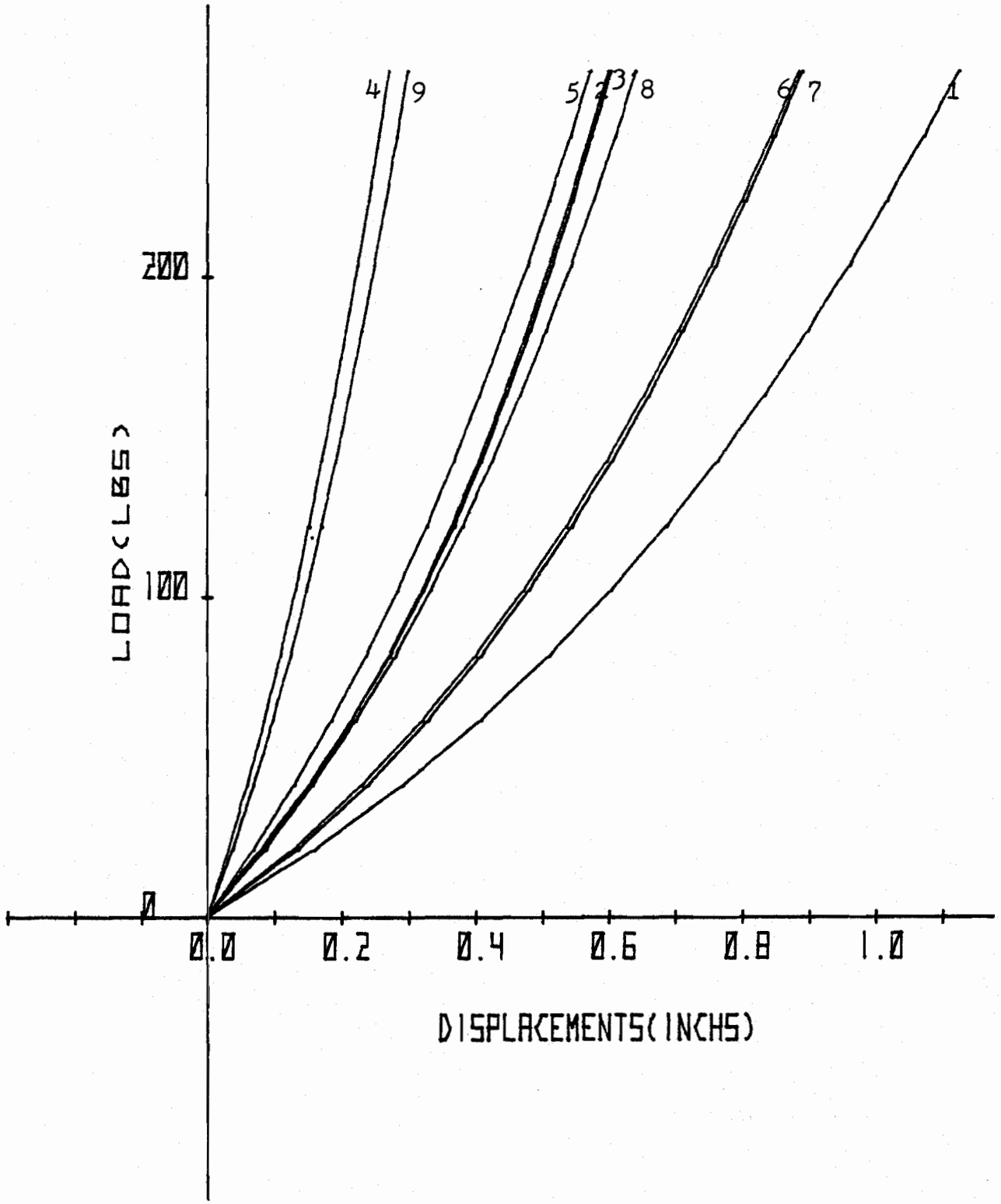

Load-displacement curves of panel no. 3A (t=0.453in.)

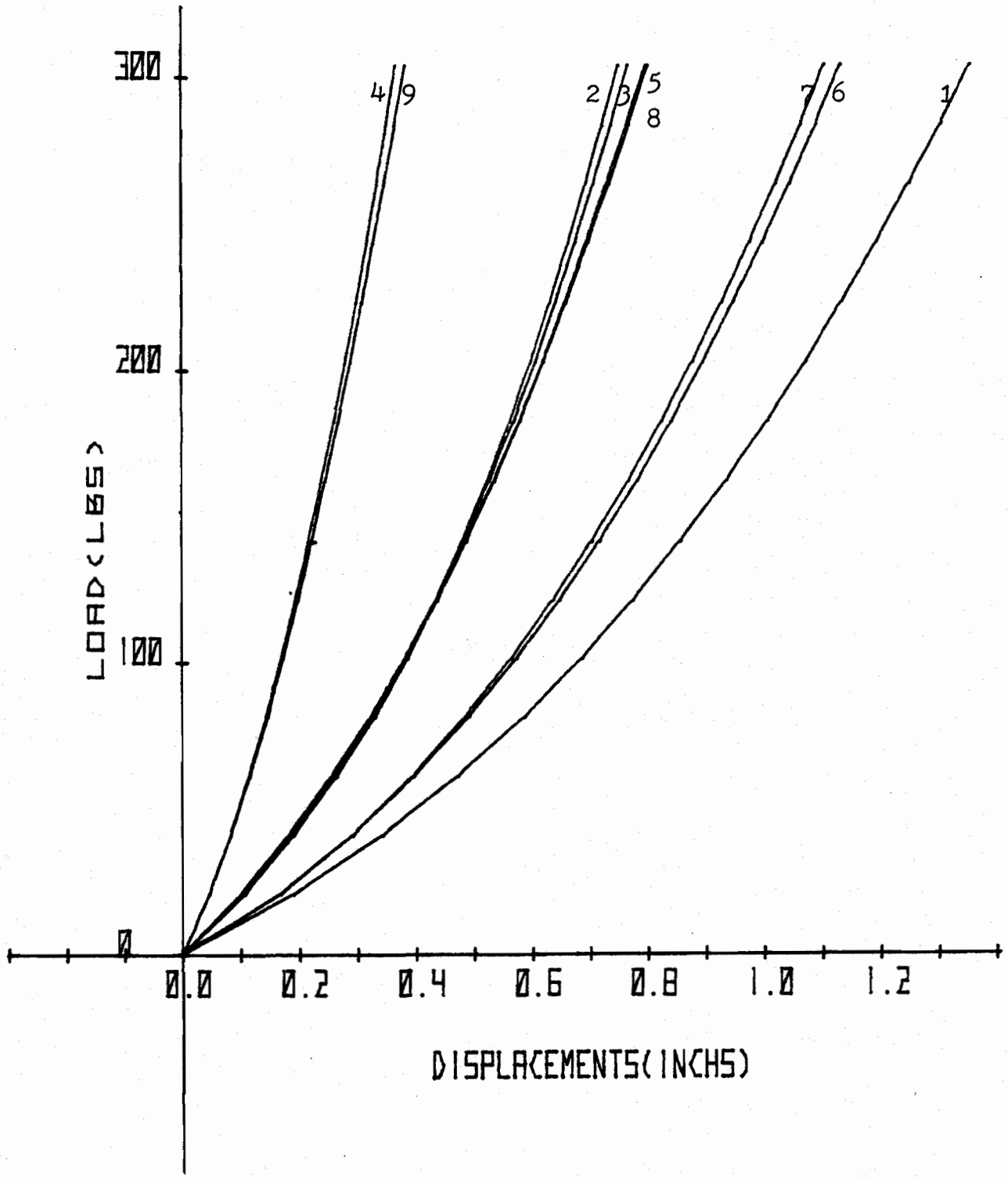

Load-displacement curves of panel no. 4A (t=0.458in.)

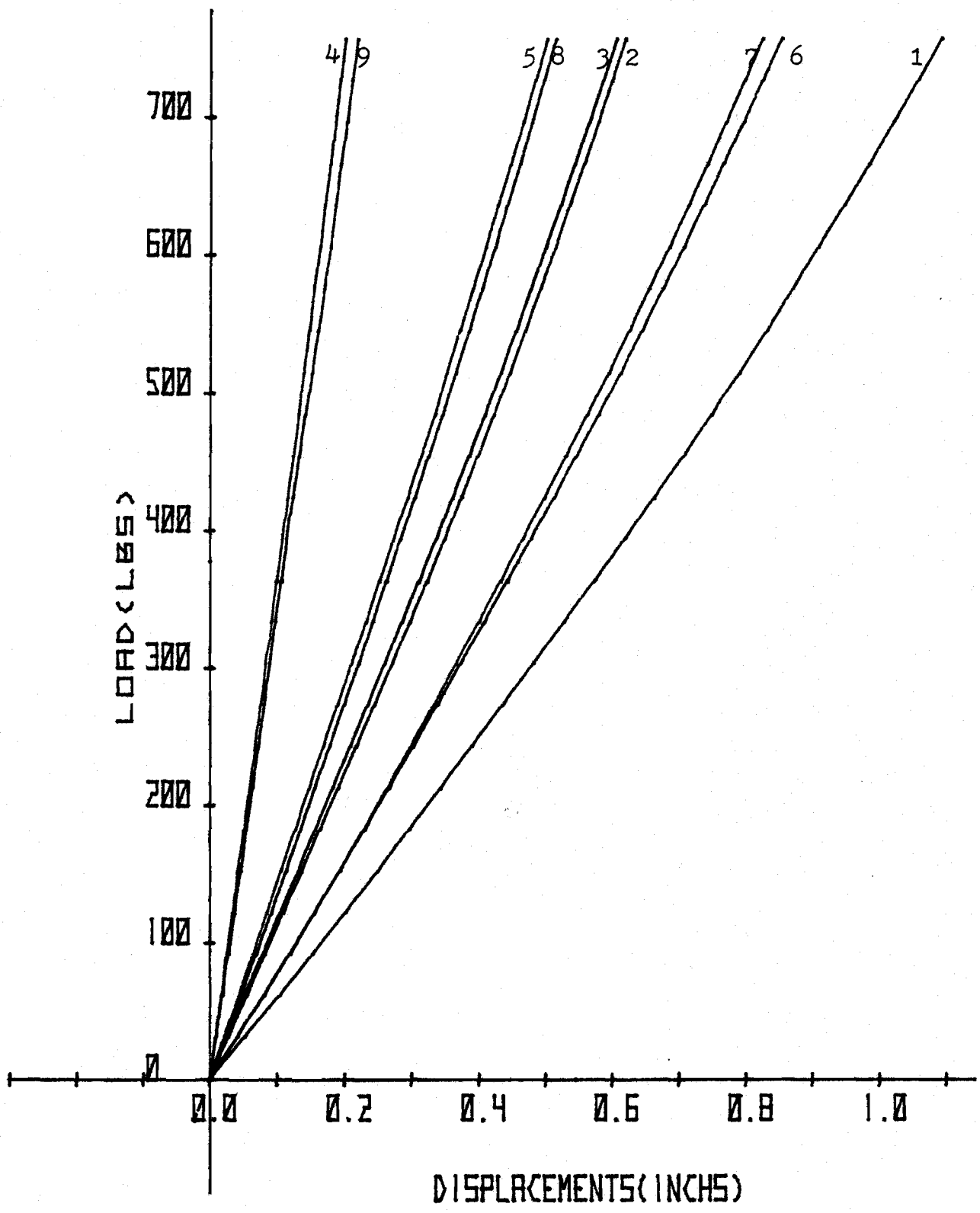

Load-displacement curves of panel no. 5A (t=0.731in.)

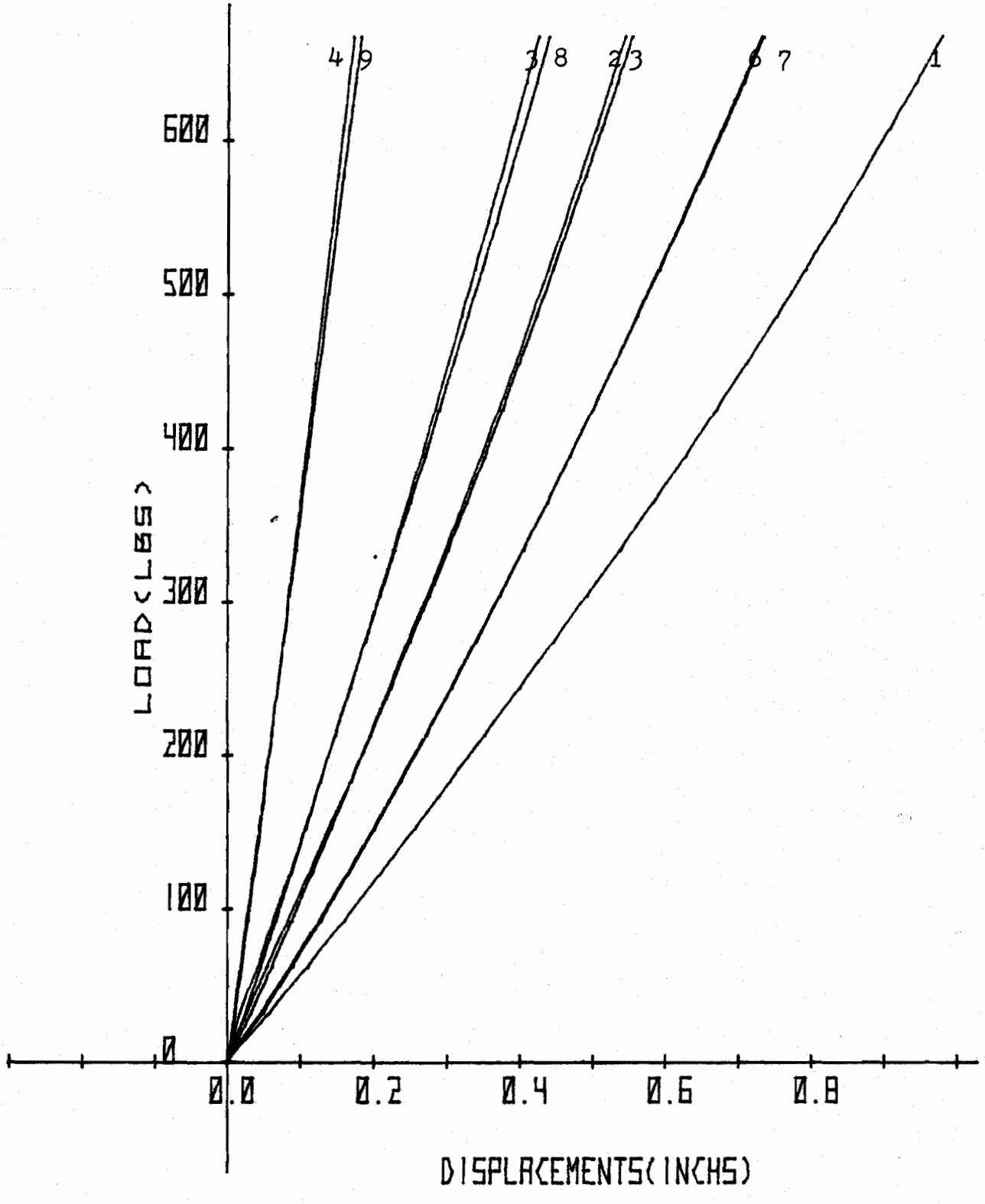

Load-displacement curves of panel no. 6A (t=0.732in.)

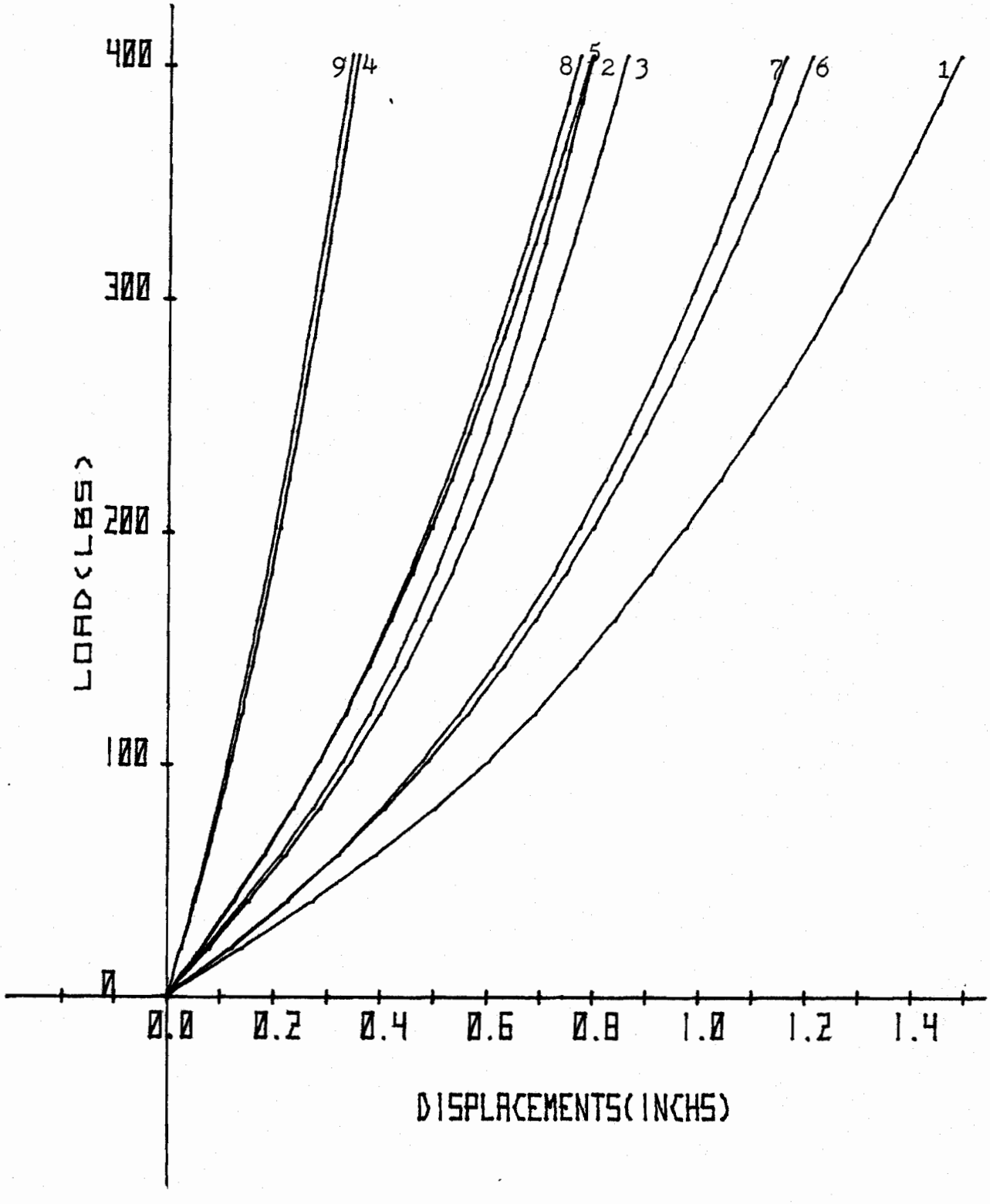

Load-displacement curves of panel no. 7A (t=0.475in.)

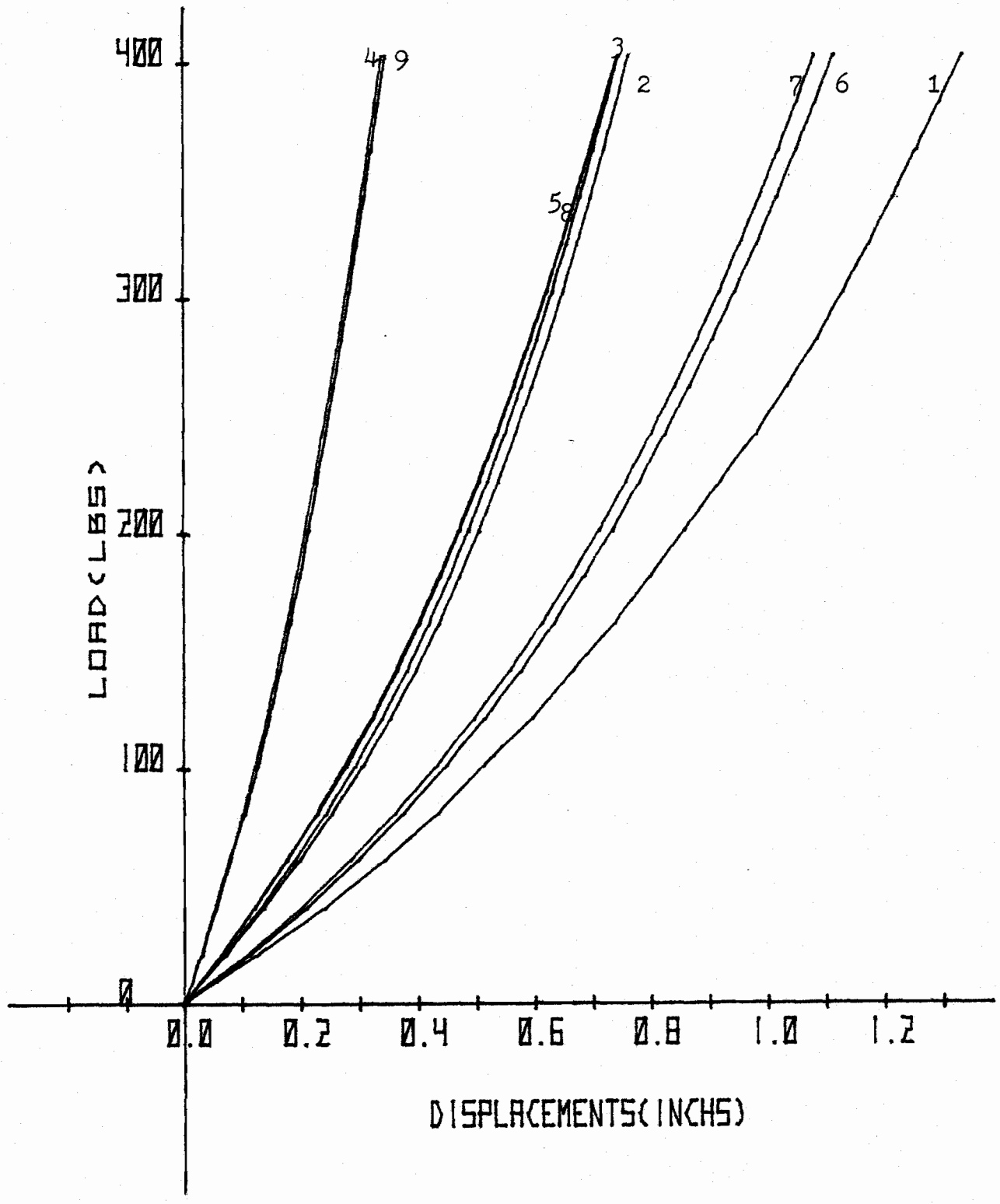

Load-displacement curves of panel no. 8A (t=0.487in.)

APPENDIX F

```
      PROGRAM PMTMOE(INPUT,OUTPUT)
C   THIS IS THE PROGRAM BEING USED TO CALCULATE THEORETICAL
C   MIDORDINATE DEFLECTION OF A PLATE UNDER PURE MOMENT
C   EX:MOE IN X-DIRECTION
C   EY:MOE IN Y-DIRECTION
C   R;EX/EY
C   A,B:PLATE DIMENSION
C   T:THICKNESS OF THE PLATE
C   PMO:UNIFORM MOMENT INTENSITY ALONG THE EDGES
C   PROGRAM CODED BY PAUL CHEN (SEPTEMBER 1980)
C
C
      READ *,EX,EY,R
      READ *,A,B,T,PMO
      PI=3.14159
      G=152.1E+3
      V=0.449
      W=V*V/R
      DX=(T**3)*EX/(12.*(1-W))
      DY=DX/R
      H=((V*EY)/(1-W)+2.*G)*(T**3)/12.
      ANG=ATAN(SQRT(DX*DY-H*H)/H)
      DO 40 I=1,3
      Y=12.*I
      FF=0.
      DO 30 M=1,9,2
      S=COS(ANG/2)*M*PI/(B*SQRT(DX))
      T=SIN(ANG/2)*M*PI/(B*SQRT(DX))
      AA=M*PI*S*A/(2*B)
      BB=M*PI*T*A/(2*B)
      F1=COSH(AA)*COS(BB)*(COS(ANG)-SIN(ANG)/(TAN(BB)*TANH(AA)))
      F2=SINH(AA)*SIN(BB)*(SIN(ANG)+COS(ANG)/(TAN(BB)*TANH(AA)))
      F0=F1-F2
      F=-SIN(M*PI*Y/B)/((M**5)*F0)
      FF=F+FF
   30 CONTINUE
      W=4*PMO*(B**4)*FF/(PI**5)
      PRINT *,W
   40 CONTINUE
      STOP
      END
 EOI ENCOUNTERED.
/BYE

AB1Q5F    LOG OFF    14.32.02.
AB1Q5F    SRU      0.674 UNTS.
```